# SPATIAL CHARACTERIZATION OF RIPARIAN BUFFER EFFECTS ON SEDIMENT LOADS FROM WATERSHED SYSTEMS

**Henrique G. Momm (corresponding author)**
henrique.momm@mtsu.edu
Assistant Professor
Department of Geosciences
Middle Tennessee State University
Murfreesboro, TN, 37132

**Ronald L. Bingner**
Agricultural Engineer
USDA-ARS-National Sedimentation Laboratory
Oxford, MS

**Yongping Yuan**
Hydrologist
U.S. – Environmental Protection Agency
Las Vegas, NV

**Martin A. Locke**
Water Quality and Ecology Research Unit
Research Leader
USDA-ARS-National Sedimentation Laboratory
Oxford, MS

**Robert R. Wells**
Hydraulic Engineer
USDA-ARS-National Sedimentation Laboratory
Oxford, MS

# SPATIAL CHARACTERIZATION OF RIPARIAN BUFFER EFFECTS ON SEDIMENT LOADS FROM WATERSHED SYSTEMS


## Abstract

Understanding all watershed systems and their interactions is a complex, but critical, undertaking when developing practices designed to reduce topsoil loss and chemical/nutrient transport from agricultural fields. The presence of riparian buffer vegetation in agricultural landscapes can modify the characteristics of overland flow promoting sediment deposition and nutrient filtering. Watershed simulation tools, such as the USDA-Annualized Agricultural Non-Point Source (AnnAGNPS) pollution model, typically require detailed information for each riparian buffer zone throughout the watershed describing the location, width, vegetation type, topography, and possible presence of concentrated flow paths through the riparian buffer zone. Research was conducted to develop GIS-based technology designed to spatially characterize riparian buffers and estimate buffer efficiency in reducing sediment loads in a semi-automated fashion at watershed scale. The methodology combines modeling technology at different scales, at individual concentrated flow paths passing through the riparian zone and at watershed scales. At the concentrated flow path scale, vegetative filter strip models can be applied to estimate the sediment trapping efficiency for each individual flow path, which are aggregated based on the watershed subdivision and used in the determination of the overall impact of the riparian vegetation at the watershed scale. This GIS-based technology is combined with AnnAGNPS to demonstrate the effect of riparian vegetation on sediment loadings from sheet and rill and ephemeral gully sources. The AnnAGNPS riparian buffer component represents an important step in understanding and accounting for the effect of riparian vegetation, existing and/or managed, in reducing sediment loads at the watershed scale.



**Keywords.** AnnAGNPS, riparian vegetation, watershed modeling, vegetative filter strips, gullies, concentrated flow

## INTRODUCTION

Targeting where to place conservation practices to reduce pollutants loads in large watershed systems involves knowing what the problem is (type and location of non-point sediment sources) and the effectiveness of one or a series of practices in controlling erosion or reducing sediment loads. The utilization of vegetative filter strips in agricultural fields has long been recognized as an effective conservation practice designed to control the amount of sediment and chemicals transported from croplands into streams, lakes, and other water bodies. This recognition is the result of numerous studies in laboratory, research plots, and field experiments; as documented by multiple authors in detailed literature reviews of a large number of research investigations assessing and quantifying the efficiency of vegetative filter strips (Liu et al., 2008; Zhang et al., 2010; Yuan et al., 2009; Osborne, et al., 1993; Wenger, 2009; Fox et al., 2013). In addition to the scientific community, conservationists and producers have also acknowledged the importance of vegetative filter strips (Petchenik, 1999). These vegetative zones are primarily designed to reduce flow velocity using various physical mechanisms such as ponding of overland flow at the upstream edge, dispersing the flow, and increasing surface roughness with above-ground vegetation. The reduced flow velocity promotes overland flow infiltration, rainfall filtration, and sediment deposition; all of which yield reduced amounts of sediment, nutrients, and pesticides exiting the system (Dillaha et al., 1989). However, the efficiency of vegetative filter strips is dependent on a complex interaction between the vegetative filter strip width perpendicular to the flow, the vegetation type, local terrain slope, soil type, and surface/subsurface flow conditions (Liu et al., 2008). Out of these parameters, buffer width, vegetation type, local topography, and surface flow characteristics have been recognized as the main parameters controlling their effectiveness (Halley, 2002) and have been adopted by modeling algorithms due to the availability of information for their estimation. These parameters are used to calculate the sediment trapping efficiency (TE), which is defined by the ratio of the mass flowing into the buffer and the mass flowing out the buffer zone (Dabney et al, 1995). Technology has been developed over the years to estimate TE as a function of key selected parameters in the form of either empirical (Yuan et al., 2009; Liu, et al., 2008) or physically-based models like the Riparian Ecosystem Management Model-REMM (Lowrance et al., 1998) and the Vegetative Filter Strip Modeling System-VFSMOD (Munoz-Carpena et al., 1999). Both of these approaches (empirical relationships and physically-based models) were designed to work on one-dimensional profiles representing small research plots or laboratory flumes. Use of such tools is therefore limited in the

estimation of the effects of riparian buffers on sediment delivery to streams and lakes at larger scales, e.g. watershed scales (Liu et al., 2007; Helmers et al., 2005).

Conversely, at the watershed scales understanding the impact of buffers that work as filter strips on improving water quality is a very difficult and complex task, as there are few technological approaches available for watershed-wide application. The interactions between different sediment sources and multiple conservation/farming practices require an integrated approach. For instance, the introduction of an edge-of-field vegetative buffer at a location upstream in the watershed can significantly reduce sediment delivery locally; however, buffer implementation could have an adverse impact on sediment production by disrupting the balance of sediment at downstream areas of the watershed (clean water effect) resulting in the production of more sediment from channel erosion sources in those downstream areas. Similarly, farming practices can influence surface flow regimes and adversely promote concentration of overland flow (concentrated flow paths); changing the hydrological regime which prevents the reduction of flow velocity and therefore change the premise that sediment is efficiently being trapped (Pankau et al., 2012). In addition to the spatial distribution pattern of overland flows exiting the cropland and entering the vegetative buffer system, another important consideration is the amount of energy present in each individual flow entering a buffer (Dosskey, et al., 2002). All these inter-related characteristics can affect the sediment trapping performance of the vegetative buffer (Baker et al., 2001).

This applies to implementing new conservation practices as well as the identification of existing riparian vegetation that has the potential to perform as managed filter strips (Pankau et al., 2012). The latter areas are an important part of the landscape, and although they can function similarly to managed riparian (streamside) areas, they are often overlooked in their role of reducing sediment loads. In a watershed system, existing riparian vegetation areas need to be evaluated for spatial connectivity and/or fragmentation because they are not designed (Bentrup and Kellerman, 2004). Verifying spatial connectivity requires assessing how buffer features upstream affect the efficiency of another buffer feature immediately downstream (buffer features organized in series, also referred to as daisy chain-coupled). The fragmentation problem constitutes the variation in buffer width and/or lack of vegetative cover of a buffer feature in a particular field and fragmentation can affect the overall sediment trapping efficiency of the entire field (buffer features organized in parallel with gaps between them). Additionally, despite the documented advantages of vegetative filter strips in reducing sediment and chemical delivery to water bodies, their implementation often comes at the cost of reduced production area. The placement of such conservation

practices should be optimized for maximum sediment trapping efficiency with minimum production disruption (Dosskey et al, 2008) while, at the same time, account for the integrated effect of all watershed systems including the contribution of existing riparian vegetation and their spatial characteristics (spatial continuity and fragmentation). Watershed conservation managers need tools to identify the most efficient and cost effective system-wide approach for improving water quality and ecosystem services (Xiang, 1996; Fox et al., 2013).

Multiple GIS and remote sensing studies exist on riparian vegetation at the watershed scale. These studies can be broadly classified according to their main objective into three groups: (i) identification and classification of existing riparian vegetation/zones using remote sensing and GIS analysis (Volkman, 2005; Goetz, 2006; Goetz et al., 2003; Abood et al.; 2012; Ilhardt, et al. 2000), (ii) optimized placement of managed riparian vegetation (Tomer et al., 2003), and (iii) integration of watershed-scale models with plot-scale riparian buffer models (Liu et al., 2008). The present study best aligns with the third group, by describing technology critical to assessing riparian buffer effectiveness for any location within a watershed system.

The main objective of this study is to develop GIS-based technology designed to spatially characterize parameters of riparian buffer zones necessary to estimate the efficiency of buffers in reducing sediment loads in a semi-automated approach at a watershed scale. This methodology was developed to link modeling technologies at two different scales, (i) buffer models applied to individual concentrated flow paths passing through the riparian vegetation zone with (ii) watershed models utilized to simulate sediment loads at individual fields and streams throughout the watershed. This integrated multi-scale GIS approach produces critical information necessary for riparian buffer models to assess the impact of riparian buffers on reducing sediment loads using a pseudo two-dimensional representation of individual concentrated flow paths. The resulting individual efficiency estimates of sets of concentrated flow paths are used to determine the overall impact of the riparian vegetation of buffers throughout the entire watershed using watershed-based simulation tools. These two procedures are described using watershed basic representation units and illustrated with a study case.

# BACKGROUND

### ANNUALIZED AGRICULTURAL NON-POINT SOURCE (ANNAGNPS) POLLUTION MODEL

The Agriculture Research Service (ARS) and the Natural Resource Conservation Service (NRCS), both branches of the U.S. Department of Agriculture, jointly developed the AGricultural Non-Point Source (AGNPS) pollution modeling system (AGNPS, Bingner and Theurer, 2001a). This technology was developed as a set of integrated tools

to evaluate the effect of conservation practices on nonpoint source pollutant loadings in agricultural watersheds and provide the necessary tools for improved watershed management decisions. A continuous-simulation, watershed-scale, mixed-land use, surface-runoff, revised version of the single event AGNPS (Young et al., 1989), referred to as the Annualized AGricultural Non-Point Source pollution model (AnnAGNPS, Bingner and Theurer, 2001b), was developed as the critical component of the updated AGNPS modeling system. AnnAGNPS is used to evaluate the long-term effect of agricultural farming and conservation practices on nonpoint source pollutants, assist with selection and spatial location of best management practices (BMPs), and evaluate the integrated effect of different farming and conservation practices. AnnAGNPS predicts the origin and movement of water, sediment, and chemicals at any location in the watershed. The model was developed with multiple components acting in concert, designed to account for different sediment source areas and sinks, and considers the impacts of conservation practices. Tracking pollutants back to their source is one of the key features the model provides to following how and where practices affect pollutant loadings from where they originate. The model is capable of distinguishing between erosion processes (i.e. sheet and rill, tillage-induced ephemeral gullies, classical and edge-of-field gullies processes) and streambed and bank sources. The model has been validated in many studies and widely applied for evaluating the impact of agricultural management practices/conservation practices on nonpoint source pollution across the world (Yuan et al., 2001; 2003; 2005; Baginska et al., 2003; Suttles et al., 2003; Licciardello et al., 2007; Shamshad et al., 2008).

In the AnnAGNPS methodology, the watershed is subdivided and characterized into basic elements of one of the two types, sub-catchment areas and channel-type concentrated flow paths; referred to as AnnAGNPS cells and AnnAGNPS reaches respectively (Figure 1A). This sub-division is often based on user-defined parameters such as the critical cell area and/or the minimum reach length, and/or combination of both values. For each of these basic elements, describing existing and antecedent conditions using a wide range of physical and environmental parameters is critical, including those conditions describing soil parameters, topographic characteristics, management practices, climate parameters, and many others. Recently, AnnAGNPS was enhanced with a riparian buffer component to quantify the contribution of existing and managed riparian vegetation in reducing transport of sediments, and consequently chemicals/nutrients, from croplands into downstream water bodies. The riparian buffer component requires the identification and detailed characterization of vegetative zones on a watershed scale for each AnnAGNPS cell and AnnAGNPS reach (Figure 1B). Consequently, the methodology introduced herein describes

riparian zones and procedures used to estimate sediment-trapping efficiency for each individual AnnAGNPS cell and AnnAGNPS reach.

## MATERIAL AND METHODS

***Development of Riparian BufferUtilization of GIS capabilities to characterize riparian buffers***

The scale gap between buffer models and watershed models is addressed by utilizing AnnAGNPS buffer (AGBUF) GIS technology designed to generate sediment trapping efficiency values for each individual AnnAGNPS cell and AnnAGNPS reach in the watershed influenced by riparian buffer zones (a GIS layer describing the geographical extent of the riparian vegetation). The proposed methodology is subdivided into two distinct methods: one for AnnAGNPS cells and another for AnnAGNPS reaches (see dashed line boxes in Figure 2).

Three GIS inputs are required for both methods: riparian zone spatial extent, land use land cover (layer with vegetation type information), and Digital Elevation Model (DEM). The DEM is initially processed using the TOPAGNPS computer program, a sub-set of the topographic parameterization (TOPAZ) computer program (Garbrecht and Martz, 1996, 1997). The computer program TOPAGNPS removes small imperfections in the DEM data, such as filling small sinks and removal of outliers, and computes multiple topographic attributes based on user provided parameters. The topographic attributes used by the AnnAGNPS riparian buffer component are flow vector, flow accumulation, terrain local slope, sub-catchments, and stream network (Figure 2). Drainage area is calculated by using the flow accumulation and the raster grid cell size.

***Trapping Efficiency Technology for Edge-of-Field (AnnAGNPS Cells) Riparian Buffers***

To aid in the description of the GIS methods, a single AnnAGNPS cell was developed for illustration purposes (Figure 3). For AnnAGNPS cell estimations of the riparian buffer impacts on sediment loads, two criteria were considered, concentrated flows that originate upstream of the riparian buffer zone and therefore passing through the riparian zone and concentrated flow paths that originate within the riparian zone. These concentrated flow paths represent the portion of the AnnAGNPS cell's overall flow affected by the riparian zone. Each concentrated flow path is used to estimate a local trapping efficiency (LTE) value through the utilization of buffer models (empirical or physically-based). The set of LTE values are aggregated into a single TE value devised to quantify the influence of the riparian buffer on sediment loads from the AnnAGNPS cell. The identification of concentrated flow profiles meeting the first criteria (flows originating upstream) begins with the identification of two key raster grid cells, the "upstream edge" and "downstream edge" raster grid cells. Upstream edge grid cells are defined as raster grid cells

located within the riparian zone that receives flow (defined as stated in box 1 in Figure 2 and identified as circles in Figure 3). Downstream edge grid cells are defined as raster grid cells located within the riparian zone with flow exiting the riparian zone (defined as stated in box 2 in Figure 2 and identified as squares in Figure 3). The concentrated flow paths between the upstream and downstream grid cells are sought to represent one-dimensional profiles and their physical characteristics are used to calculate local sediment trapping efficiencies for each flow path (see inset in Figure 3). Sediment-trapping efficiency values are estimated using either empirical or physically-based riparian buffer models. Herein, empirical relationships are used for simplicity; however, the proposed GIS framework could be adopted without major changes to work with physically-based models. For each of the profiles, the contributing drainage area at the upstream edge and at the downstream edge grid cells, flow path length, profile average slope, and dominating vegetation cover type are determined (defined as stated in box 3 in Figure 2). Profiles are referred to by identifiers composed of the AnnAGNPS cell identification plus a unique numerical identifier.

A single representative sediment trapping efficiency value for each AnnAGNPS cell is calculated by aggregating local sediment trapping efficiency value from all concentrated flow-paths; originating in and upstream of the riparian zone. For the concentrated flow paths passing through the riparian zone, individual local sediment trapping efficiencies are calculated using the equations 2, 3, and 4 (defined as stated in box 4 in Figure2) as derived from Yuan et al. (2009).

$$TE_{local} = 0.6261 * ([W_f])^{0.127}$$ ; vegetation = grass-type AND buffer slope $\leq$ 0.05 m/m [2]

$$TE_{local} = 0.6747 * ([W_f])^{0.060}$$ ; vegetation = grass-type AND buffer slope $>$ 0.05 m/m [3]

$$TE_{local} = 0.5957 * ([W_f])^{0.1327}$$ ; vegetation = bushes and forest [4]

In these equations, $W_f$ is the effective buffer width, which is estimated by the concentrated flow path length. In the case of grass-type vegetation, the average slope of the concentrated flow path is used to determine which trapping efficiency model is employed.

Any flow originating within the riparian zone is defined as having a local sediment trapping efficiency (LTE) of one, since the assumption is that sediment is not detached and transported from within the riparian buffer zone. In the AnnAGNPS cell described, eleven concentrated flow paths originating within the riparian buffer zone are identified (diamonds in Figure 4A) and associated with points of concentrated flow 3, 4, 5, 6, 7, 9, 10, 11, 12, 13, 16 (Figure 3).

Although the profiles representing the concentrated flow paths originated within the riparian zone are assumed to have a LTE of 1, they represent only a small fraction of the total flow generated by the AnnAGNPS cell. The effect of these concentrated flow paths needs to be reflected in the overall AnnAGNPS cell overall trapping efficiency. Therefore, the contributions of all individual flow paths originating within the riparian buffer zone are scaled using the drainage areas of the most downstream raster grid cell each flow path and the total AnnAGNPS cell drainage area (box 4 Figure 2). Downstream edge grid cells with flow originating within the buffer zone are identified (diamonds in Figure 4) and their contribution to the overall AnnAGNPS TE is determined using:

$$TEC_W = \sum_{i=1}^{n} \left( \frac{LTE_i * DA_{ds_i}}{DA_{cell}} \right) \quad [5]$$

where $LTE$ is the local trapping efficiency for concentrated flow into downstream edge raster grid cell *i* and $DA_{ds_i}$ is the drainage area for the downstream edge raster grid cell *i* and $DA_{cell}$ is total drainage area of the AnnAGNPS cell. Calculations of the contribution of these LTE values to the overall AnnAGNPS cell TE for the example AnnAGNPS cell for the six different scenarios, three spatial coverage extents (Figure 4A-C), and two vegetation types are listed in Table 1.

Similar calculations are performed for concentrated flow passing through the riparian zone. However, because some of the downstream edge raster grids receive flow from more than one concentrated flow path, individual local sediment trapping efficiency values need to be combined using a weighted average procedure based on drainage area values of the upstream edge raster grids (circles in Figure 4). This calculation is exemplified for the left-most downstream edge raster grid (left-most square in Figure 4C); which receives flow from three concentrated flow paths (Table 2). This method allows for the calculation of a single local trapping efficiency value for each downstream edge raster grid associated with points of concentrated flow 1, 2, 8, 14, 15, 17, 18 (Figure 3). Similarly to the flow originated inside the buffer zone, these values are then expressed in terms of their contribution to the overall AnnAGNPS cell TE using the equation:

$$TEC_C = \sum_{i=1}^{n} \left( \frac{ALTE_i * DA_{ds_i}}{DA_{cell}} \right) \quad [6]$$

where $ALTE$ is the adjusted local trapping efficiency for concentrated flow into downstream edge raster grid cell *i* and $DA_{ds_i}$ is the drainage area for the downstream edge raster grid cell *i* and $DA_{cell}$ is total drainage area of the

AnnAGNPS cell. Calculations of the contribution of LTE values estimated for each concentrated flow path passing through the riparian zone to the overall AnnAGNPS cell TE trapping efficiency for the AnnAGNPS example cell for six different scenarios are listed in Table 3. The overall sediment trapping efficiency of the AnnAGNPS cell is then the summation of the contribution from the flows within and through the AnnAGNPS cell as illustrated in Table 4.

***Concentrated Flow that the Riparian Vegetative Buffer Does Not Effect (Short-Circuit)***

Among the designed properties of vegetative buffers is the ability to disperse and reduce the velocity of the surface flow through the buffer. However, in natural occurring riparian vegetation, above-ground vegetation might not slow flow velocities as result of large stream flows (flow energy). This excess in energy can be the result of high precipitation, steep slopes, topography-induced flow concentration (convex surfaces), and, most commonly, generated by large drainage areas. An example of such phenomena is the presence of tillage-induced ephemeral gullies (Figure 5). To account for concentrated flows "short-circuiting" the riparian buffer, an alternative based on the upstream drainage area was introduced. The user has the option to provide a drainage area threshold value, which is compared to the drainage area of the upstream raster grid cell of each flow profile. If the drainage area of a flow profile is greater than the threshold value provided, the local trapping efficiency is set to zero and the calculations proceed as described in the previous section. The AGBUF technology has been integrated with the AGNPS Potential Ephemeral Gully (PEG) technology (Momm et al., 2012) providing an integrated approach to assessing conservation practices impacting tillage and ephemeral gully erosion with the capability of buffers to remove sediment as simulated with AnnAGNPS.

***Trapping Efficiency Technology for In-Stream (AnnAGNPS Reaches) Riparian Buffers***

Sediment transported to locations represented as AnnAGNPS reaches can also be affected by the presence of vegetative buffers (Figure 6). AnnAGNPS reaches are internally defined as one-dimensional features and the following assumption was considered in the evaluation of their effect on sediment trapping efficiency. The riparian zone has to extend in width perpendicular to the flow direction of least half of the raster grid cell size on both sides of the AnnAGNPS reach. Alternatively, the user has the option of providing a minimum width value greater than one half of the raster grid cell size.

A simplified schematic is used to describe the AnnAGNPS reach methodology (Figure 6). The initial step is the identification of "valid" raster grid cells along the reach. These valid raster grid cells must meet the width

requirements previously described and be located within a riparian zone (box 6 in Figure 2). The same nomenclature of downstream and upstream edge raster grid cells used in AnnAGNPS cells calculations are adopted herein.

The procedure starts by identifying and marking upstream and downstream edge raster grid cells (box 7 in Figure 2). The AnnAGNPS reach is evaluated from upstream to downstream. Raster grid cells located in the riparian buffer and receiving flow from upstream raster grid cells outside of the riparian buffer (edge cells) are temporarily identified. Next, the conditions of having a left and right raster grid cells (perpendicular to the flow direction) based on the provided minimum width are then determined. If these conditions are not met, then this cell is not designated an upstream edge grid cell and the next downstream raster grid cell is then temporarily identified as an upstream edge grid cell. This procedure is repeated until all conditions are met. Similar procedures are applied for the characterization of downstream edge raster grid cells. Although, if the conditions are not met, the next upstream cell is temporarily identified (Figure 6B) and the procedure recursively repeated.

For example, in Figure 6B the most northern dashed line represents the case where the reach raster grid cell is within the buffer zone and receiving flow from raster grid cells outside of the buffer zone. However, this particular raster grid cell was not considered in the buffer zone as a result of containing only one neighbor raster grid cell (perpendicular to the flow direction). Conversely, the subsequent raster grid cell is then identified as downstream edge cell. The same evaluation procedure is performed for the identification of the downstream edge raster grid cells (most southern dashed line in Figure 6B).

If a reach raster grid cell is located within the buffer zone and is receiving flow from upstream while flowing outside the buffer zone, the grid cell is classified as both an upstream and downstream edge cell (hexagonal in Figure 6C).

Differently from the AnnAGNPS cell-based approach previously described, in the AnnAGNPS reach-based approach the user-provided drainage area threshold is not used. Information on peak discharge and channel geometry parameters are utilized internally by the AnnAGNPS model to determine the reduction of the vegetative buffer efficiency when high-energy flows are present, also referred to as short circuits. In addition, while in the AnnAGNPS cell-based approach the AGNPS riparian buffer component reports one value of trapping efficiency, buffer width, and slope for each AnnAGNPS cell, the AnnAGNPS reach-based approach of AGBUF reports these parameters for each riparian buffer that the AnnAGNPS reach passes through. In other words, for the case of multiple buffer zones along an AnnAGNPS reach, individual parameters for each buffer zone are reported. The

justification for this approach is that buffer zones located in AnnAGNPS reaches are in series and therefore the outcome of one influences the performance of another located downstream. The AnnAGNPS model also performs these interactions between multiple buffer zones located within the same AnnAGNPS reach internally.

# EXAMPLE OF WATERSHED APPLICATION

## WATERSHED DESCRIPTION

The Goodwin Creek Experimental Watershed (GCW) is located near Batesville, Mississippi (Figure 7A), in the Bluff Hills physiographic subprovince just east of the Mississippi River Alluvial Valley and is characterized by steep slopes and highly erodible soils. The USDA-ARS National Sedimentation Laboratory (NSL) has been monitoring the hydrology and sediment transport of the GCW since 1981. The GCW stream flow infrastructure consists of supercritical flow stream gauge stations, with 14 stations located throughout the 21.3 $km^2$ area representing the whole of Goodwin Creek (Figure 7B). The GCW is a mixed land use watershed that contains row crop agriculture, pasture, and forest (Kuhnle et al, 2008). Agriculture production has declined over the years and crops have been replaced by forest and pasture. The watershed precipitation is dominated by high rainfall producing winter and spring frontal storms, with widely scattered and variable thunderstorms during the summer, all significantly influenced by Gulf of Mexico fronts. Annual precipitation averaged approximately 1340 mm/yr between 1981--2010. Average daily high air temperatures range from 10° C to greater than 30° C with average daily low temperatures from 0° C to 20° C in the winter and summer months, respectively.

### *Assessment of Riparian Buffer Effects Using AnnAGNPS Simulations*

The effect of different riparian vegetation properties, characterized by AGBUF, on sediment load reduction was evaluated using multiple AnnAGNPS simulations. The watershed simulated was a subset of the Goodwin Creek Watershed with the outlet defined downstream of stream gage 14 (Figure 7C). This subwatershed was subdivided into 213 AnnAGNPS cells and 86 AnnAGNPS reaches, but to illustrate the buffer technology and for better description of the analysis and subsequent interpretation of the results, only three AnnAGNPS cells (141,142, and 143) and one AnnAGNPS reach (14) are depicted (Figure 7D) herein and in the subsequent sections.

A digital elevation model (DEM) with spatial resolution of 1-m generated from an airborne LiDAR survey was used to describe the topography and generate the necessary topographic parameters. This DEM was pre-processed through an iterative procedure to remove man-made features not represented by the raw DEM, such as individual property culverts and small bridges. The pre-processed DEM was analyzed using the TOPAGNPS computer

program to generate the needed input files in raster grid file format for the AnnAGNPS buffer component: watershed subdivision, flow vectors, stream network, flow accumulation, and terrain local slope (Figure 2).

AnnAGNPS simulations of the sub-watershed from gauging station 14 (Figure 7C) were developed (930,000 $Mg.year^{-1}$) and compared to observed average annual streamflow (940,000 $Mg.year^{-1}$) from 1982 to 1995. The main sources of sediment for this watershed were comprised of sheet and rill erosion, ephemeral gully erosion, and stream bank erosion. Total sediment load simulated by AnnAGNPS was 2700 Mg/year, in comparison to observed total sediment load of 1860 $Mg.year^{-1}$.

Visual inspection of aerial photographs acquired in 1979, 1985, and 1996 was performed to identify and map existing riparian vegetation and ephemeral gully locations (Figure 7D). The existing riparian vegetation zone (primarily forest vegetation) affecting the three AnnAGNPS cells reported has a varying buffer width and directly affects the sediment loads from AnnAGNPS reach 14 and AnnAGNPS cells 142 and 143 (Figure 8). Two potential ephemeral gully initiation points (most downstream point for gully channel initiation) were identified based on evaluation of aerial photographs and the compound topographic index (CTI) analysis using the AnnAGNPS potential ephemeral gully component (Momm et al., 2012). These ephemeral gully initiation points are marked as red squares in Figure 8.

The inclusion of ephemeral gullies as sources of sediment in the simulations were sought to demonstrate the integrated capabilities between AGNPS components, as the transport and delivery of ephemeral gully sediment loads to downstream locations are influenced by the presence of riparian vegetation in the flow path of the gully. Whether the gully initiation point is located within the riparian vegetation zone or is located upstream of the riparian vegetation zone greatly impacts how the ephemeral gully is going to evolve and regenerate sediment for transport to streams and lakes.

***Effects of Vegetation Cover Type on Sediment Loads***

Five AnnAGNPS simulations were performed by varying the vegetation cover type. In addition to the existing riparian vegetation identified during the aerial photograph inspection, a second riparian zone was included (light green in Figure 8). This riparian zone is referred to as “managed” and is designed to represent the implementation of vegetation riparian buffers as an effective conservation practice. The five vegetation cover types considered include, (i) no existing or managed riparian vegetation zones, (ii) existing forest, (iii) existing managed, (iv) existing forest and managed grass, and (v) existing and managed forest (Figure 8).

### *Effects of the Riparian Zone Spatial Extent on Sediment Loads*

Varying the extent of the managed riparian zone allowed for the assessment of the effects of the riparian zone spatial extent on sediment loads. The vegetation types selected were forest and grass for the existing and managed riparian zones, respectively. The managed riparian zone width values considered were 5, 10, 20, and 40 meters (Figure 9). The integrated effect of sediment loads generated by ephemeral gullies with the varying riparian zone extent was accounted for in all four AnnAGNPS simulations.

### *Effects of Concentrated Flow Through Riparian Zone on Sediment Loads*

A third investigation focused on the presence of concentrated flow paths with high stream powers that would significantly reduce the capability of the riparian buffer to retain sediment generated upstream. The vegetation type used was forest for the existing riparian zone and grass for the managed riparian zone (Figure 8). The drainage area threshold values considered were 50, 250, 1,000, 2,000, and 5,000 $m^2$. Threshold values were compared to the drainage area of individual raster grid cells marked as upstream edge cells (edge raster grid cells receiving flow from upstream). Highlighting the drainage area of upstream edge cells is important and is determined by accumulating all drainage areas of the raster grid cells outside of the riparian zone that flow into the selected raster grid cell (Figure 10). If an upstream edge raster grid cell has a drainage area greater than the threshold drainage area selected then that flow path through the riparian zone is simulated as a “short-circuit” with no trapping efficiency designated (red circles in Figure 10).

## RESULTS AND DISCUSSION

### *Effects of Vegetation Cover Type on Sediment Loads*

The change in management from production to idle fields starting in 1992 affected sediment load estimations by the AnnAGNPS model, and this change is noted in the reduction in sediment levels from previous months (Figure 11). Each vegetation cover scenario affects sediment loads from individual sources differently. Inspection of sediment loads produced by sheet and rill erosion indicates a significant increase in sediment retention when considering only existing vegetation as vegetative buffer strips (Figure 12A). The AnnAGNPS simulation that considered only the existing buffer (forest and grass vegetation types) estimated sediment loads to be approximately 43% of the sediment loads when no riparian zone was considered. With the addition of a managed riparian zone,

AnnAGNPS results indicated an 87% sediment load reduction with a small reduction in productive area could be achieved. This is an obvious impact from the buffer width as predicted by the buffer models utilized at each concentrated flow path. Additionally, small differences were reported between the two predominant vegetation types considered, grass and forest (Table 5).

The simulated effect of the different land cover types was more pronounced when comparing sediment load amounts from ephemeral gully sources (Figure 12B). In the study site, two gully initiation points were considered (Figure 8). With the scenario of no riparian zone, both gully initiation points (also referred to as gully headcut locations) significantly eroded since the riparian buffer vegetation was not present at their initiation point to prevent the growth of the gully. The simulation results indicate that the existing downstream riparian vegetation trapped 87% of sediments produced by ephemeral gullies. In the two scenarios that considered existing and managed riparian zones, one of the gully headcuts was spatially located within the riparian zone, and therefore the gully components within the AnnAGNPS model would not be used to predict any gully evolution in terms of headcut migration, incision, and sidewall expansion. The second (upstream) gully headcut was estimated to have no effect on sediment production because this flow path was estimated to have a local trapping efficiency of 100%. However, the AnnAGNPS model still reported sediment loads from ephemeral gully erosion (Figure 12B), as particles sizes are influenced differently by the vegetative filter strip. The sediment loads reported when both existing and managed gullies were present represent particles of clay size, which are assumed to be in suspension and therefore not trapped by the riparian buffer (Figure 12C).

***Effects of the Riparian Zone Spatial Extent on Sediment Loads***

Similar to the vegetation type investigation, there were differences in the sediment load estimated from each sediment source considered (Figure 13). For sheet and rill erosion estimates, increasing riparian width up to 20 meters reduced sediment loads, as the simulated scenario with 40 meters yielded similar results to the 20 meters wide riparian zone (Figure 13A and Table 6). Comparable estimations between the 20 and the 40 meters scenarios agree with experimental plot results in which the first upstream meters are the most effective portion of the riparian filter strip (Yuan et al. 2009; Zhang et al., 2010). This was also reflected in the empirical relationships considered (buffer models), as they were expressed using power functions, which tend to produce a constant effect beyond certain width values.

Sediment load estimates from ephemeral gullies were the same for riparian zones of 10, 20, and 40 meters, where the 5 meter riparian zone width produced minimal sediment (Figure 13B). The downstream ephemeral gully initiation point was located within the riparian zone and did not evolve for either of the 10, 20, and 40 meters width scenarios. While the upstream gully initiation point was spatially located outside of the riparian zone for the 20 meters width scenario, all sediment produced was trapped in the downstream vegetative buffer. In the 40 meters width scenario, both gully initiation points were located within the riparian zone and they did not evolve. Although, the AnnAGNPS model still produced a small amount of sediment load resulting from suspended eroded clay particles. Ephemeral gully contribution to sediment production was higher at the 5 meters width scenario in which both gully initiation points were located outside of the riparian zone and therefore predicted to fully evolve. Thus, the ephemeral gully sources had a greater impact on total sediment load (Figure 13B-C and Table 6).

***Effects of Concentrated Flow Through Riparian Zone on Sediment Loads***

Evaluating the effect of concentrated flow paths within riparian filter strips required identifying individual concentrated flow paths that have high levels of stream power energy and therefore would significantly reduce the capability of the riparian filter strip to retain sediment generated upstream. The drainage area threshold values considered were 50, 250, 1,000, 2,000, and 5,000 $m^2$ for forest conditions in the existing riparian zone and grass for the managed riparian zone (Figure 8). The use of drainage area threshold is intended to capture and simulate high-energy flows that limit the ability of the riparian filter strip to slow and to spread the surface flow. Using small threshold values result in more concentrated flow paths being considered as "short circuits" and having no effect in reducing sediment loads (Figure 14A). An important consideration is that all scenarios in this evaluation had the same spatial extent (riparian zone widths were the same), but produced significant differences in sediment trapping efficiency values between scenarios and between AnnAGNPS cells. When no threshold value was used, AnnAGNPS cells 141, 142, and 143 were estimated to have similar values of sediment trapping efficiency. As the threshold value was reduced from 5,000 to 50 $m^2$, these cells produced different sediment trapping efficiency values. This difference highlights distinct surface flow patterns within each AnnAGNPS cell. Cells 141 and 143 had concentrated flows containing a wide range of drainage areas, while for AnnAGNPS cell 142, most of the concentrated flow paths contained drainage areas smaller than 250 $m^2$.

The effect of short circuits was more pronounced for sediment loads generated from ephemeral gully erosion (Figure 14B). In the scenario that no drainage area threshold was utilized, (blue line in Figure 14B), most of the

sediment was either not produced (gully does not form) or was trapped by the riparian filter strip and only small amounts of sediment were transported to the reach in the form of diluted clay. With the introduction of the threshold values, the concentrated flow path where both gully initiation points were located was considered a short circuit and therefore all sediment produced by these gullies was estimated as being transported into the reach. The effect of these short circuits was highlighted when comparing sediment loads from simulation scenarios with and without riparian vegetation and varying drainage area threshold values (Figure 13C and Table 7).

## SUMMARY AND CONCLUSIONS

A GIS-based framework was described to characterize riparian buffer vegetation in a distributed fashion to estimate their effects on reducing sediment loads transported from agricultural uplands into downstream water bodies. This technology helps to bridge the gap between one-dimensional plot and/or field scale buffer models and watershed-scale erosion models, such as the USDA-AnnAGNPS model. Parameters of individual concentrated flow paths through the riparian buffer zone were quantified and utilized as input for buffer models in the estimation of local sediment trapping efficiency values. Sediment trapping efficiency values for each AnnAGNPS basic unit (AnnAGNPS cells and AnnAGNPS reaches) was obtained by weighted aggregation methods of a set of sediment trapping efficiency values. The AnnAGNPS model estimated sediment-trapping efficiency for individual ranges of particle sizes, as filter strips affect them differently.

The AnnAGNPS buffer technology provides the capability to evaluate the impact of concentrated flow paths through the riparian zone, which has the potential of reducing the effectiveness of filter strips. Concentrated flow paths can automatically be determined by defining drainage area thresholds required to form concentrated flow, which then affects the local trapping efficiency of that particular concentrated flow path.

An important feature sought in modern watershed modeling and management tools is the ability to simulate the integrated effect of watershed systems and ecosystems services. Conservation and novel farming practices can have a positive effect locally on water quality, but sometimes results in unintended consequences elsewhere in the watershed. This is a key feature of the AnnAGNPS buffer GIS technology in which the integrated potential effects of riparian vegetation in reducing sediment loads from multiple sources are implemented with the sources tracked to their origin, as demonstrated in this study by the evaluation of sediment loads from sheet and rill and ephemeral gullies.

The AnnAGNPS buffer GIS technology has been developed to serve as a template to determine the required information needed for existing models, empirical relationships and/or physically based models and can be used with new models/relationships for sediment trapping efficiency that may be developed. As a result, future developments of this technology will include the estimation of surface flow information for each individual flow path through and within the buffer, which could the utilization of additional physical-based models, such as VSFMOD and REMM, in the estimation of local trapping efficiency. Additionally, at the present stage of development, the AnnAGNPS buffer GIS tool records buffer information on individual flow paths and individual buffers through reaches, allowing users to utilize this information in their own relationships and therefore, overwrite the calculated sediment trapping efficiency.

Also, as the understanding of the integrated effects between riparian vegetation and wetlands continues to evolve, future enhancements within AnnAGNPS will include quantifying this interaction, as both are common ecosystem conservation practices and often are employed together.

Furthermore, in these studies, GIS layers with the riparian zone extent and vegetation type (land cover map) were used. These layers were generated from digitization of such information from multiple years of high resolution aerial photograph datasets. This requires tedious and time consuming efforts, especially for large watersheds. The development of technology needed is anticipated to derive this information in a semi-automated way from remotely sensed sources such as high-resolution satellite imagery or LiDAR data.

Finally, the utilization of vegetative filter strips is considered an important, effective and efficient conservation practice that has been shown to protect ecosystem services at field-scales, but their full impact on the watershed-scale is still subject to ongoing research. The AGBUF technology developed within AGNPS provides researchers and watershed conservation managers the capability to evaluate the placement of conservation practices, track the loads to their source, and assess their system-wide efficiency on improving water quality and ecosystem services.

## REFERENCES


Abood, S.A, A.L. Maclean, L.A. Mason, 2012. Modeling Riparian Zones Utilizing DEMS and Flood Height Data. Photogrammetric Engineering and Remote Sensing, 78(3): 259-269.

Baginska, B., W. Milne-Home, and P.S. Cornish. 2003. Modeling nutrient transport in Currency Creek, NSW with AnnAGNPS and PEST. Environ. Model. Softw. 18:801-808.

Baker, M.E., M.J. Wiley, and P.W. Seelbach, 2001. GIS-based hydrologic modeling of riparian areas: implications for stream water quality, Journal of the American Water Resources Association, 37(6): 1615-1628.

Bentrup, G. and T. Kellerman, 2004. Where should buffers go? Modeling riparian habitat connectivity in northeast Kansas. Journal of Soil and Water Conservation, 59(5): 209-215.

Bingner, R.L. and F.D. Theurer, 2001a. AGNPS 98: A Suite of water quality models for watershed use. In Proceedings of the Sedimentation: Monitoring, Modeling, and Managing, 7th Federal Interagency Sedimentation Conference, Reno, NV. p. VII-1 - VII-8.

Bingner, R.L. and F.D. Theurer, 2001b. AnnAGNPS: estimating sediment yield by particle size for sheet & rill erosion. In Proceedings of the Sedimentation: Monitoring, Modeling, and Managing, 7th Federal Interagency Sedimentation Conference, Reno, NV. p. I-1 - I-7.

Dabney, S.M., L.D. Meyer, W.C. Harmon, and C.V. Alonso, 1995. Depositional patterns of sediment trapped by grass hedges. Transactions of the ASABE, 38(6): 1719-1729.

Dillaha, T.A., R.B. Reneau, S. Mostaghimi, and D. Lee, 1989. Vegetative filter strips for agricultural nonpoint source pollution control. Transactions of the ASAE, 32(2): 513–519.

Dosskey, M.G., M.J. Hemlers, D.E. Eisenhauer, 2008. A design aid for determining width of filter strips. Journal of Soil and Water Conservation, 63(4): 232-241.

Dosskey, M.G., M.J. Hemlers, D.E. Eisenhauer, T.G. Franti, and K.D. Hoagland, 2002. Assessment of concentrated flow through riparian buffers. Journal of Soil and Water Conservation, 57(6): 336-343.

Fox, G.A., C.J. Penn, 2013. Empirical model for quantifying total phosphorus reduction by vegetative filter strips. Transactions of the ASABE, 56(4): 1461-1469.

Garbrecht, J., and L.W. Martz, 1997. The assignment of drainage direction over flat surfaces in raster digital elevation models. J. Hydrol. 193(1): 204-213.

521 Garbrecht, J., and L.W. Martz, 1996. Digital landscape parameterization for hydrological applications. In HydroGIS
522 96: Application of Geographic Information Systems in Hydrology and Water Resources Management, 169-
523 174. IAHS Publ. No. 235. International Association of Hydrological Sciences.
524 Goetz, S.J., R.K. Wright, A.J. Smith, E. Zinecker, and E. Schaub, 2003. IKONOS imagery for resource
525 management: Tree cover, impervious surfaces, and riparian buffer analyses in the mid-Atlantic region. Remote
526 Sensing of Environment. 88: 195–208
527 Goetz, S.J., 2006. Remote Sensing of Riparian Buffers: Past Progress and Future Prospects. Journal of the
528 American Water Resources Association (JAWRA). 42(1): 133-143.
529 Halley, J.M., 2002. Watershed management and Riparian Buffer Analyses using Remotely Sensed Data, Graduate
530 Thesis, North Carolina State University, North Carolina, USA.
531 Helmers, M.J., D.E. Eisenhauer, T.G. Franti, and M.G. Dosskey, 2005. Modeling Sediment Trapping In A
532 Vegetative Filter Accounting For Converging Overland Flow. Transactions of the ASAE, 48(2): 541-555.
533 Ilhardt, B.L., E.S. Verry and B.J. Palik, 2000. Defining Riparian Areas, Riparian Management in Forests of the
534 Continental Eastern United States. (Verry, E.S., J.W. Hornbeck and C.A. Dolloff ,editors). Lewis Publishers,
535 New York, NY, pp. 23-42.
536 Kuhnle, R.A., R.L. Bingner, C.V. Alonso, C.G. Wilson, and A. Simon, 2008. Conservation Practice Effects on
537 Sediment Load in the Goodwin Creek Experimental Watershed. Journal of Soil and Water Conservation.
538 63(6): 496-503.
539 Licciardello, F., D.A. Zema, S.M. Zimbone, and R.L. Bingner. 2007. Runoff and Soil Erosion Evaluation by the
540 AnnAGNPS Model in a Small Mediterranean Watershed. Transactions of the ASAE 50(5): 1585-1593.
541 Liu X., X. Zhang, and M. Zhang, 2008. Major Factors Influencing the Efficacy of Vegetated Buffers on Sediment
542 Trapping: A Review and Analysis. J. Environ. Qual. 37:1667–1674.
543 Liu, Y., W. Yang, and X. Wang, 2007. GIS-Based Integration of SWAT and REMM for Estimating Water Quality
544 Benefits of Riparian Buffers in Agricultural Watersheds. Transactions of the ASABE. 50(5): 1549-1563.
545 Lowrance, R.R., L.S. Altier, R.G. Williams, S.P. Inamdar, D.D. Bosch, J.M. Sheridan, D. L. Thomas, and R.K.
546 Hubbard, 1998. The riparian ecosystem management model: simulator for ecological processes in riparian
547 zones, First Federal Interagency Hydrologic Modeling Conference, April 19-23, Las Vegas, NV.

548 Momm, H., R.L. Bingner, R.R. Wells, and D. Wilcox, 2012. AnnAGNPS GIS-based tool for watershed-scale
549 identification and mapping of cropland potential ephemeral gullies. Applied Engineering in Agriculture. 28(1):
550 17-29.
551 Munoz-Carpena, R., J.E. Parsons, and J.W. Gilliam, 1999. Modeling hydrology and sediment transport in vegetative
552 filter strips, Journal of Hydrology, 214: 111-129.
553 Osborne L. L. and D. A. Kovacic, 1993. Riparian vegetated buffer strips in water-quality restoration and stream
554 management. Freshwater Biology. 29: 243-258.
555 Petchenik, J., 1999. The National Conservation Buffer Initiative – A Qualitative Evaluation. Applied Research
556 Systems Inc. Madison, WI. 55pp.
557 Pankau, R.C., J.E. Schoonover, K.W.J. Williard, P.J. Edwards, 2012. Concentrated flow paths in riparian buffer
558 zones of southern Illinois, Agroforest Syst. 84:191–205
559 Shamshad, A., C.S. Leow, A. Ramlah, W.M.A. Wan Hussin, and S.A. Mohd Sanusi. 2008. Applications of
560 AnnAGNPS model for soil loss estimation and nutrient loading for Malaysian conditions. Int. J. Appl. Earth
561 Obs. 10:239–252.
562 Suttles, J.B., G. Vellidis, D. Bosch, R. Lowrance, J.M. Sheridan, and E.L. Usery. 2003. Watershed-scale simulation
563 of sediment and nutrient loads in Georgia Coastal Plain streams using the Annualized AGNPS model. Trans.
564 ASAE 46:1325-1335.
565 Tomer, M.D., D.E. James, and T.M. Isanhart, 2003. Optimizing the placement of riparian practices in a watershed
566 using terrain analysis. Journal of Soil and Water Conservation. 58(4): 198-206.
567 Volkman, S., 2005. Quickbird Satellite Imagery for Riparian Management: Characterizing Riparian Filter Strips
568 and Detecting Concentrated Flow in an Agricultural Watershed. Master Thesis, Michigan Technological
569 University.
570 Wenger, S., 1999. A review of the scientific literature on riparian buffer width, extent and vegetation, Technical
571 Report published by the Institute of Ecology, University of Georgia Athens.
572 Xiang W., 1996. GIS-based riparian buffer analysis: injecting geographic information into landscape planning,
573 Landscape and Urban Planning, 34: 1-10.
574 Young, R.A., C.A. Onstad, D.D. Bosch, and W.P. Anderson, 1989. AGNPS: A non-point source pollution model
575 for evaluating agricultural watersheds. J. Soil & Water Conserv. 44(2): 168-173

576 Yuan, Y., R.L. Bingner, and R.A. Rebich. 2001. Evaluation of AnnAGNPS on Mississippi Delta MSEA
577 Watersheds. Transactions of the ASAE 44(5): 1183-1190.
578 Yuan, Y., R L. Bingner, and R.A. Rebich. 2003. Evaluation of AnnAGNPS Nitrogen Loading in an Agricultural
579 Watershed. Journal of AWRA 39(2): 457-466.
580 Yuan, Y., R.L. Bingner, F D. Theurer, R A. Rebich, and P A. Moore. 2005. Phosphorus Component in
581 AnnAGNPS. Transactions of the ASAE 48(6): 2145-2154.
582 Yuan, Y., R.L. Bingner, and M.A. Locke, 2009. A Review of Effectiveness of Vegetative Buffers on Sediment
583 Trapping in Agricultural Areas. Ecohydrology. 2: 321-336.
584 Zhang, X., X. Liu, M. Zhang, and R.A. Dahlgren, 2010. A Review of Vegetated Buffers and a Meta-analysis of
585 Their Mitigation Efficacy in Reducing Nonpoint Source Pollution. J. Environ. Qual. 39:76–84.

# FIGURE CAPTIONS

**Figure 1.** Illustration of the AnnAGNPS characterization of the watershed into streams and sub-catchments referred to as AnnAGNPS reaches (blue) and AnnAGNPS cells (red), respectively (A). Existing riparian vegetation zone (edge of field) in each AnnAGNPS cell is identified and characterized for improved calculations of sediment loads (B).

**Figure 2.** Schematic of the steps performed by the AGNPS riparian buffer component to estimate the effect of riparian vegetation on sediment loads for individual AnnAGNPS cells and reaches. Filled boxes indicate user-provided input information.

**Figure 3.** GIS characterization of riparian zones. Black lines passing through the buffer zone represent concentrated flow paths (simulated as one-dimensional profiles) and black raster grid cells represent AnnAGNPS reach locations. Circles represent "upstream edge" raster grid cells indicating flow into the riparian zone and squares represent "downstream edge" raster grid cells indicating flow exiting the riparian zone.

**Figure 4.** Distinction of downstream edge raster grid cells between flows that enter from outside the filter strip (squares represent the most downstream raster grid cell of these flows) and flows that begin inside the filter strip (diamonds represent the most downstream raster grid cell of these flows) for a riparian zone extent completely across the cell area that connects to a reach (A), partially across the cell (B), and is completely across the cell area and with reduced width (C).

**Figure 5.** Aerial view of concentrated flow path "short-circuiting" the riparian vegetation buffer. Concentrated flows with high energy as result of steep slopes and/or large drainage area tend to sustain high velocities reducing, or even vanishing, the sediment trapping efficiency of riparian vegetative filter strips.

**Figure 6.** Schematic of GIS analysis performed for the estimation of sediment trapping efficiency when reaches go through riparian vegetation zones.

**Figure 7.** Geographical location of the site selected for demonstrating the AnnAGNPS riparian buffer component. The site is located in the State of Mississippi (A) and represents a subset of the Goodwin Creek Experimental Watershed (B). The outlet was selected downstream of station 14 (C) but results are only reported for reach 14 (blue line in D) and for AnnAGNPS cells 141, 142, and 143 (red polygons in D)

**Figure 8.** Simulated scenarios considered in the evaluation of the vegetation type on the AnnAGNPS riparian buffer component estimation of sediment loads.

**Figure 9.** Simulated scenarios considered in the evaluation of the riparian buffer width on the AnnAGNPS riparian buffer component estimation of sediment loads.

**Figure 10.** Simulated scenarios considered in the evaluation of the presence of concentrated flow paths with high energy (short-circuits) on the AnnAGNPS riparian buffer component estimation of sediment loads.

**Figure 11.** Sediment load downstream of reach 14 generated from sheet and rill sources from the AnnAGNPS simulation without riparian vegetation.

**Figure 12.** Accumulated sediment load downstream of reach 14 generated from sheet and rill (A), ephemeral gully (B), and all combined sources (C) for each of the five simulated vegetation cover type scenarios for the riparian buffer zones**.**

**Figure 13.** Accumulated sediment load downstream of reach 14 generated from sheet and rill (A), ephemeral gullies (B), and all sources (C) for each of the four simulated buffer width scenarios.

**Figure 14.** Accumulated sediment load downstream of reach 14 generated from sheet and rill (A), ephemeral gullies (B), and all sources (C) for each of the six simulated drainage area thresholds ($m^2$) considered.

642
643

**Table 1.** Calculations of the sediment TE contribution of all concentrated flow originated within the riparian zone to the overall AnnAGNPS cell TE (Figure 4). A weighted average based on the ratio of drainage area of each concentrated flow path to the total AnnAGNPS cell drainage area[a] was used to calculate the contribution to the overall AnnAGNPS cell TE.

| Coverage A | | | Coverage B | | | Coverage C | | |
|---|---|---|---|---|---|---|---|---|
| **Flow ID num[b]** | **Down DA ($m^2$)** | **ITEC[a] F/G** | **Flow ID num[b]** | **Down DA ($m^2$)** | **ITEC[a] F/G** | **Flow ID num[b]** | **Down DA ($m^2$)** | **ITEC[a] F/G** |
| 3 | 212.18 | 0.58% | 3 | 212.18 | 0.58% | 3 | 212.18 | 0.58% |
| 4 | 212.18 | 0.58% | 4 | 212.18 | 0.58% | 4 | 212.18 | 0.58% |
| 5 | 212.18 | 0.58% | 5 | 212.18 | 0.58% | 5 | 212.18 | 0.58% |
| 6 | 212.18 | 0.58% | 6 | 212.18 | 0.58% | 6 | 212.18 | 0.58% |
| 7 | 212.18 | 0.58% | 7 | 212.18 | 0.58% | 7 | 212.18 | 0.58% |
| 9 | 212.18 | 0.58% | 9 | 212.18 | 0.58% | 9 | 212.18 | 0.58% |
| 10 | 318.27 | 0.87% | 10 | 318.27 | 0.58% | 10 | 318.27 | 0.87% |
| 11 | 106.09 | 0.29% | 11 | 106.09 | 0.58% | 11 | 106.09 | 0.29% |
| 12 | 1060.9 | 2.90% | 12 | 318.27 | 0.58% | 13 | 212.18 | 0.58% |
| 13 | 212.18 | 0.58% | | | | 16 | 318.27 | 0.87% |
| 16 | 318.27 | 0.87% | | | | | | |
| **Total TE Contribution** | | **8.99%** | | | **5.51%** | | | **6.09%** |

Down DA – Drainage area at downstream raster grid cells (diamonds in Figure 4).
F/G – Equal TE contribution values for forest and grass vegetation types.
ITEC – Individual Trapping Efficiency Contribution.
[a] Total Cell Drainage Area: 36,601.05 $m^2$.
[b] Concentrated flow paths originated within each of the three riparian zones considered in Figure 4A to 4C. Most downstream raster grid cell in these flow paths are represented as diamonds (Figure 4). Numbering schema is from left to right hand-side (Figure 3).

644
645
646
647

**Table 2.** Illustration of local trapping efficiency estimation when downstream edge raster grid receives flow from more than one concentrated flow path. Depicted in this table is left most downstream edge raster of Figure 4C.

| Flow ID Number | Flow Length (m) | Flow Path Average Slope (m/m) | Local TE Grass | Local TE Forest | Upstream Edge Drainage Area ($m^2$) | Weight |
|---|---|---|---|---|---|---|
| 1A | 49.73 | 0.002 | 1.000 | 1.000 | 848.72 | 0.138 |
| 1B | 35.17 | 0.005 | 0.984 | 1.000 | 2,121.80 | 0.345 |
| 1C | 14.57 | 0.001 | 0.880 | 0.897 | 3,182.70 | 0.517 |
| | | | | Total Upstream Edge Drainage Area | 6,153.20 | |
| | | | | | Adjusted Local Trapping Efficiency Grass | 0.932 |
| | | | | | Adjusted Local Trapping Efficiency Forest | 0.947 |

652
653

**Table 3.** Calculations of the sediment TE contribution of all concentrated flow originated outside the buffer zone to the overall AnnAGNPS cell TE (Figure 4). A weighted average based on the ratio of drainage area of each concentrated flow path to the total AnnAGNPS cell drainage area[a] was used to calculate the contribution to the overall AnnAGNPS cell TE.

| | Flow ID Number[b] | Downstream DA ($m^2$) | Adjusted LTE forest | Adjusted LTE grass | Individual TE contribution[a] forest | Individual TE contribution[a] grass |
|---|---|---|---|---|---|---|
| Coverage A (Figure 4A) | 1 | 7001.94 | 1.000 | 1.000 | 19.13% | 19.13% |
| | 2 | 2652.25 | 1.000 | 1.000 | 7.25% | 7.25% |
| | 8 | 4349.69 | 1.000 | 1.000 | 11.88% | 11.88% |
| | 14 | 7850.66 | 1.000 | 1.000 | 21.45% | 21.45% |
| | 15 | 1273.08 | 1.000 | 1.000 | 3.48% | 3.48% |
| | 17 | 5516.68 | 1.000 | 1.000 | 15.07% | 15.07% |
| | 18 | 4667.96 | 0.999 | 1.000 | 12.74% | 12.75% |
| | | | **Total TE Contribution** | | **91.00%** | **91.01%** |
| Cov. B (Fig. 4B) | 1 | 7001.94 | 1.000 | 1.000 | 19.13% | 19.13% |
| | 2 | 2652.25 | 1.000 | 1.000 | 7.25% | 7.25% |
| | 8 | 4349.69 | 1.000 | 1.000 | 11.88% | 11.88% |
| | | | **Total TE Contribution** | | **38.26%** | **38.26%** |
| Coverage C (Figure 4C) | 1 | 7001.94 | 0.932 | 0.947 | 17.84% | 18.11% |
| | 2 | 2652.25 | 0.844 | 0.868 | 6.12% | 6.29% |
| | 8 | 4349.69 | 0.880 | 0.897 | 10.46% | 10.66% |
| | 12 | 1060.9 | 0.460 | 0.473 | 1.33% | 1.37% |
| | 14 | 7850.66 | 0.966 | 0.981 | 20.72% | 21.05% |
| | 15 | 1273.08 | 0.766 | 0.788 | 2.67% | 2.74% |
| | 17 | 5516.68 | 0.897 | 0.915 | 13.52% | 13.79% |
| | 18 | 4667.96 | 0.920 | 0.945 | 11.73% | 12.06% |
| | | | **Total TE Contribution** | | **84.37%** | **86.06%** |

Downstream DA - Drainage area at downstream raster grid cells (squares in Figure 4).

[a] Total Cell Drainage Area: 36,601.05 $m^2$.

[b] Concentrated flow paths originated outside each of the three riparian zones considered in Figure 4A to 4C. Most downstream raster grid cell in these flow paths are represented as squares (Figure 4). Numbering schema is from left to right hand-side (Figure 3).

654
655
656

**Table 4.** Representative sediment trapping efficiency value for AnnAGNPS cell 403.

| | Contribution to the overall AnnAGNPS cell TE | | | | | |
|---|---|---|---|---|---|---|
| | **A-forest** | **A-grass** | **B-forest** | **B-grass** | **C-forest** | **C-grass** |
| Flow Inside Buffer | 8.99% | 8.99% | 5.51% | 5.51% | 6.09% | 6.09% |
| Flow Outside Buffer | 91.00% | 91.01% | 38.26% | 38.26% | 84.37% | 86.06% |
| **AnnAGNPS cell TE** | **99.98%** | **100.00%** | **43.77%** | **43.77%** | **90.46%** | **92.15%** |

662
663
664 **Table 5.** Sediment trapping efficiency values for AnnAGNPS simulations varying vegetation type of riparian
665 buffers.

| Scenarios | Cells | | | Reach 14 |
|---|---|---|---|---|
| | 141 | 142 | 143 | Effective TE* |
| existing forest and managed forest | 99% | 92% | 97% | 92% |
| existing forest and managed grass | 96% | 92% | 97% | 91% |
| existing grass | n/a | 82% | 76% | 66% |
| existing forest | n/a | 90% | 79% | 68% |
| no riparian vegetation | n/a | n/a | n/a | n/a |

* average annual sediment load from all sources ratio between each AnnAGNPS simulation scenario and AnnAGNPS simulation with no riparian vegetation.

666

667
668
669 **Table 6.** Sediment trapping efficiency values for AnnAGNPS simulations varying vegetation type of riparian
670 buffers.

| Scenarios | Cells | | | Reach 14 |
|---|---|---|---|---|
| | 141 | 142 | 143 | Effective TE* |
| 5 meters | 72% | 90% | 82% | 79% |
| 10 meters | 81% | 91% | 90% | 86% |
| 20 meters | 85% | 92% | 97% | 90% |
| 40 meters | 100% | 92% | 92% | 91% |

* average annual sediment load from all sources ratio between each AnnAGNPS simulation scenario and AnnAGNPS simulation with no riparian vegetation.

671
672
673
674

675
676
677 **Table 7.** Sediment trapping efficiency values for AnnAGNPS simulations varying the drainage area threshold of
678 riparian vegetative buffers.

| Scenarios | Cells | | | Reach 14 |
|---|---|---|---|---|
| | 141 | 142 | 143 | Effective TE* |
| 50 | 3% | 38% | 20% | 38% |
| 250 | 4% | 69% | 32% | 44% |
| 1,000 | 18% | 92% | 35% | 47% |
| 2,000 | 44% | 92% | 55% | 58% |
| 5,000 | 96% | 92% | 55% | 63% |
| No threshold | 96% | 92% | 97% | 91% |

* average annual sediment load from all sources ratio between each AnnAGNPS simulation scenario and AnnAGNPS simulation with no riparian vegetation.

679
680
681

682
683

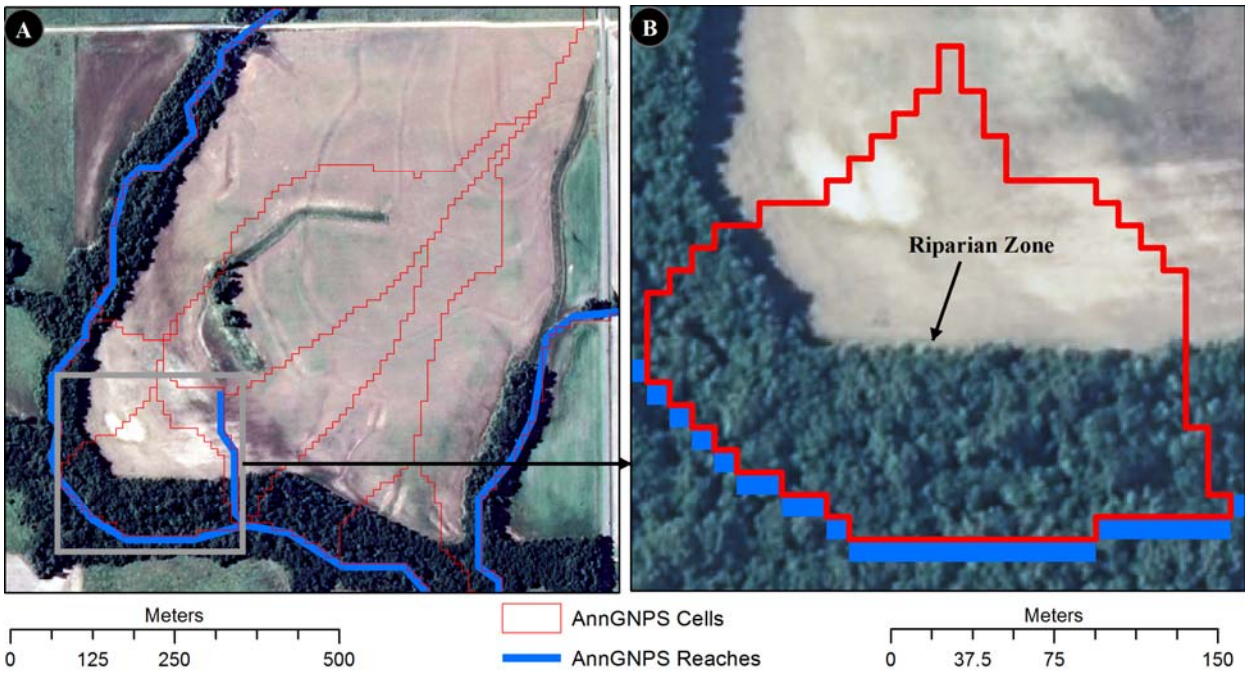


**Figure 1.** Illustration of the AnnAGNPS characterization of the watershed into streams and sub-catchments referred to as AnnAGNPS reaches (blue) and AnnAGNPS cells (red), respectively (A). Existing riparian vegetation zone (edge of field) in each AnnAGNPS cell is identified and characterized for improved calculations of sediment loads (B).

684
685
686
687
688

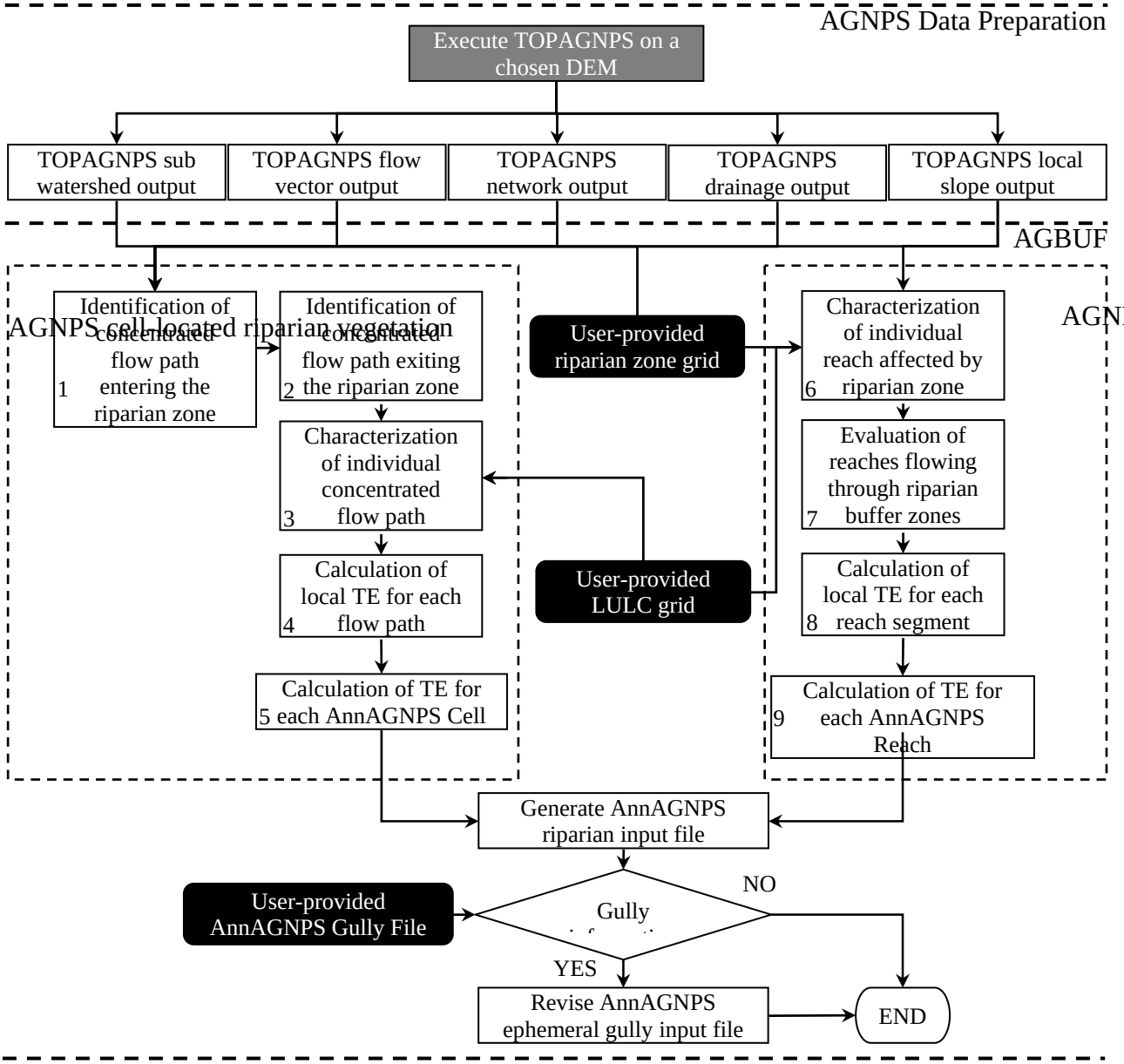


**Figure 2.** Schematic of the steps performed by the AGNPS riparian buffer component to estimate the effect of riparian vegetation on sediment loads for individual AnnAGNPS cells and reaches. Filled boxes indicate user-provided input information.

691
692

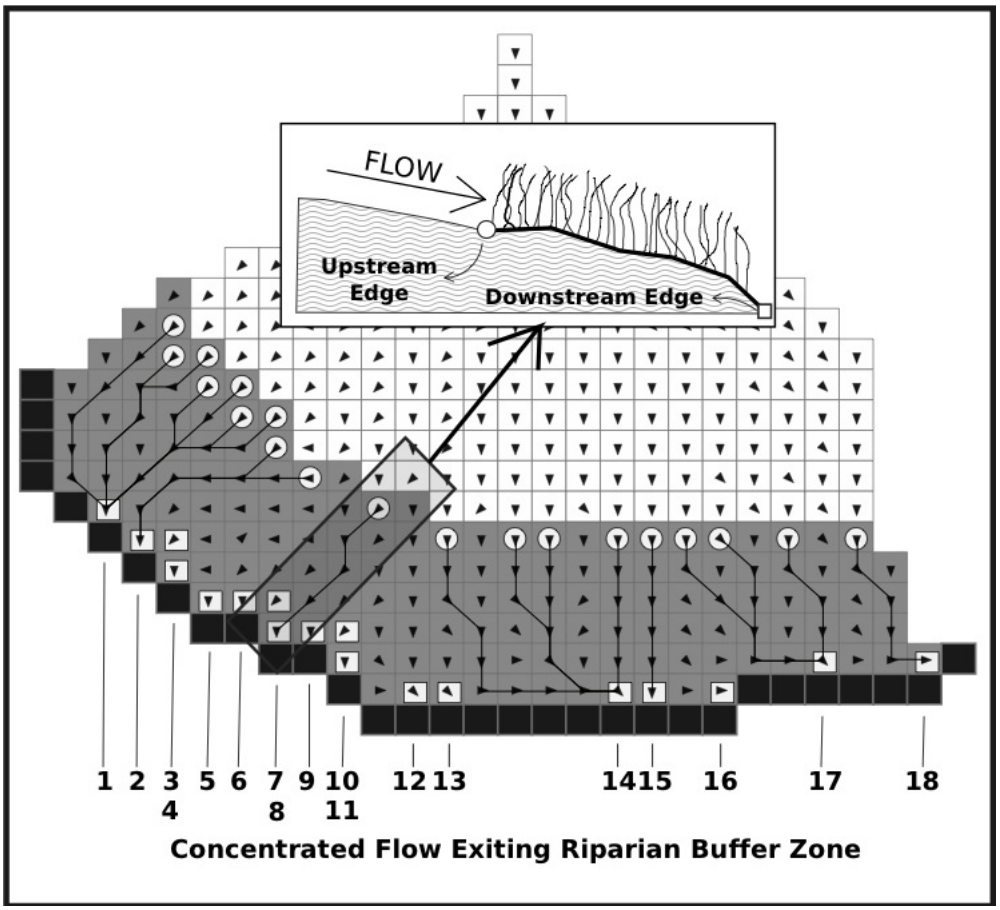


**Figure 3.** GIS characterization of riparian zones. Black lines passing through the buffer zone represent concentrated flow paths (simulated as one-dimensional profiles) and black raster grid cells represent AnnAGNPS reach locations. Circles represent "upstream edge" raster grid cells indicating flow into the riparian zone and squares represent "downstream edge" raster grid cells indicating flow exiting the riparian zone.

693
694

695

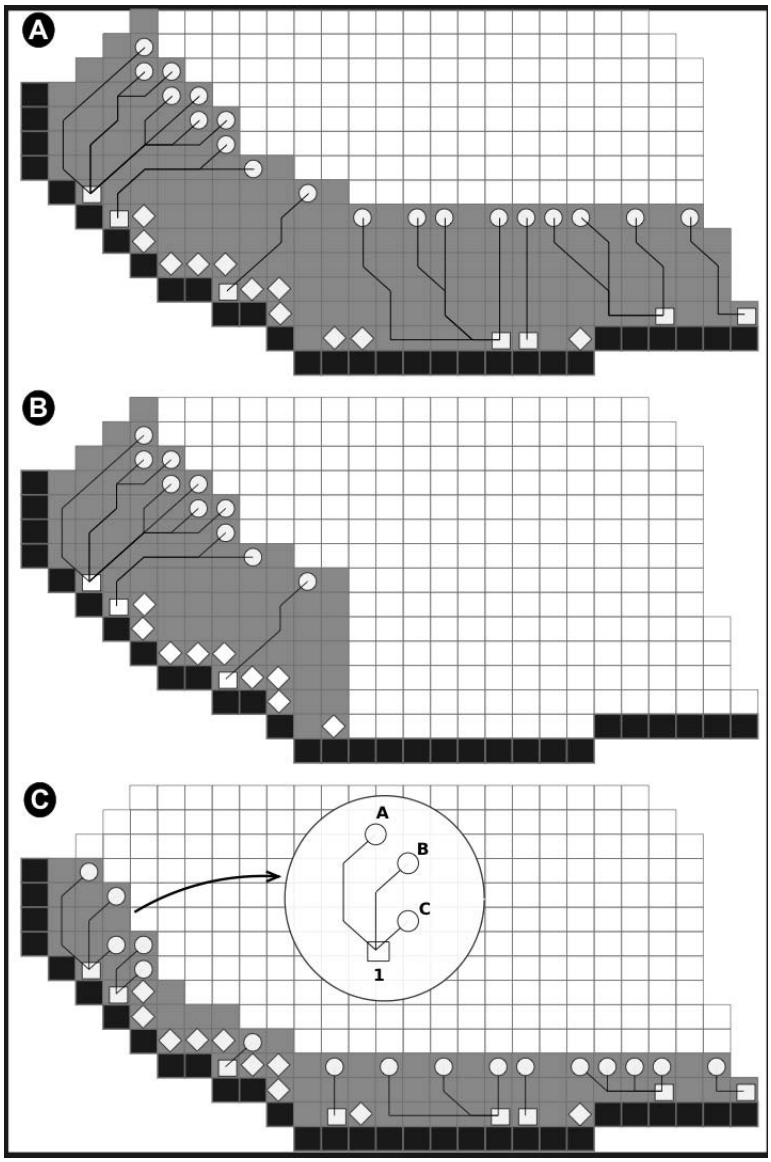


**Figure 4.** Distinction of downstream edge raster grid cells between flows that enter from outside the filter strip (squares represent the most downstream raster grid cell of these flows) and flows that begin inside the filter strip (diamonds represent the most downstream raster grid cell of these flows) for a riparian zone extent completely across the cell area that connects to a reach (A), partially across the cell (B), and is completely across the cell area and with reduced width (C).

696
697

698

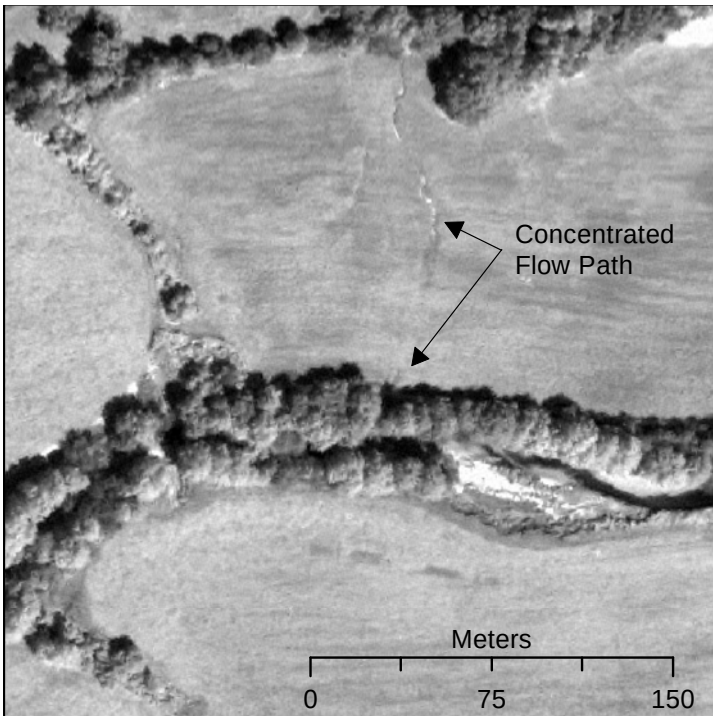


**Figure 5.** Aerial view of concentrated flow path "short-circuiting" the riparian vegetation buffer. Concentrated flows with high energy as result of steep slopes and/or large drainage area tend to sustain high velocities reducing, or even vanishing, the sediment trapping efficiency of riparian vegetative filter strips.

699

700

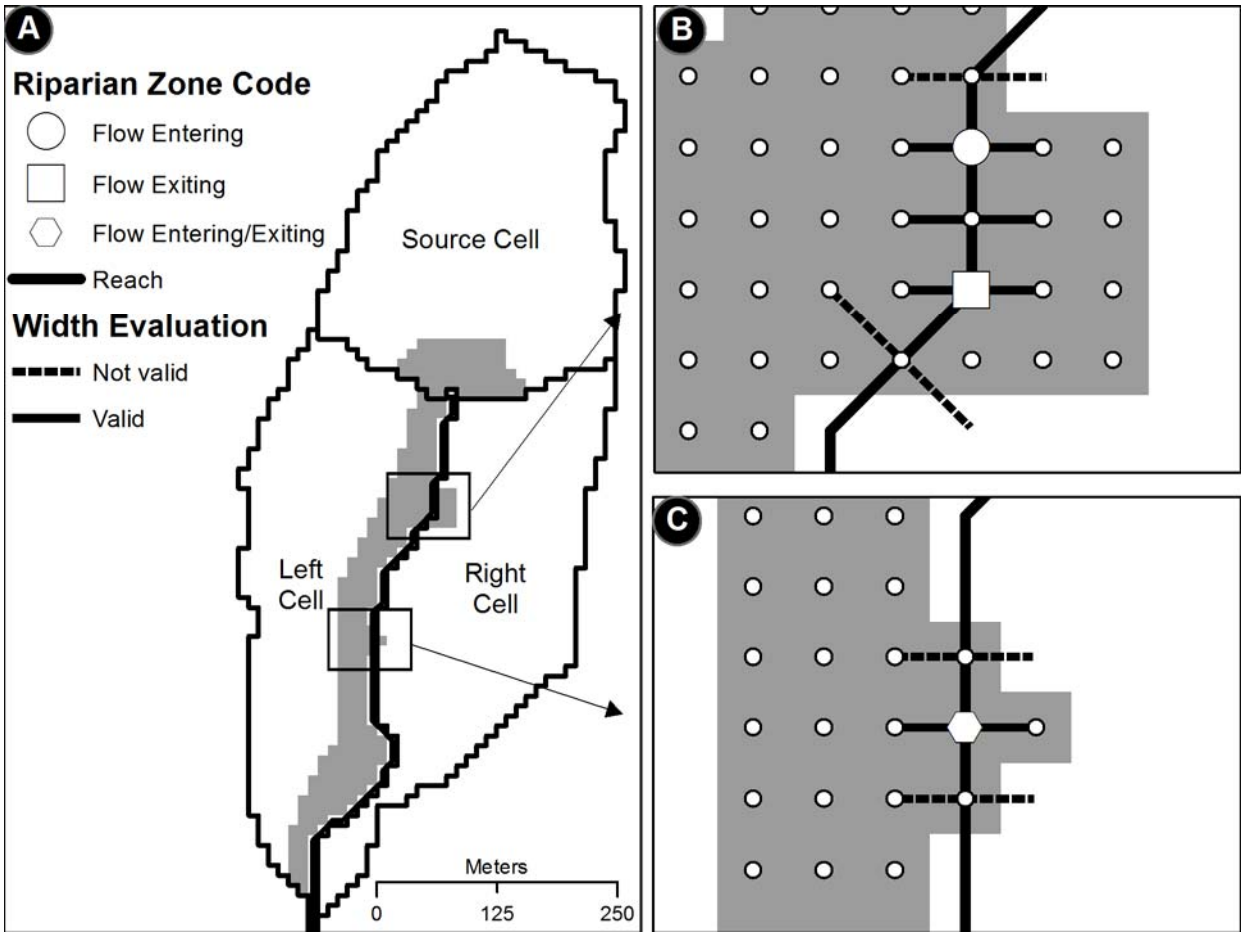


**Figure 6.** Schematic of GIS analysis performed for the estimation of sediment trapping efficiency when reaches go through riparian vegetation zones.

701

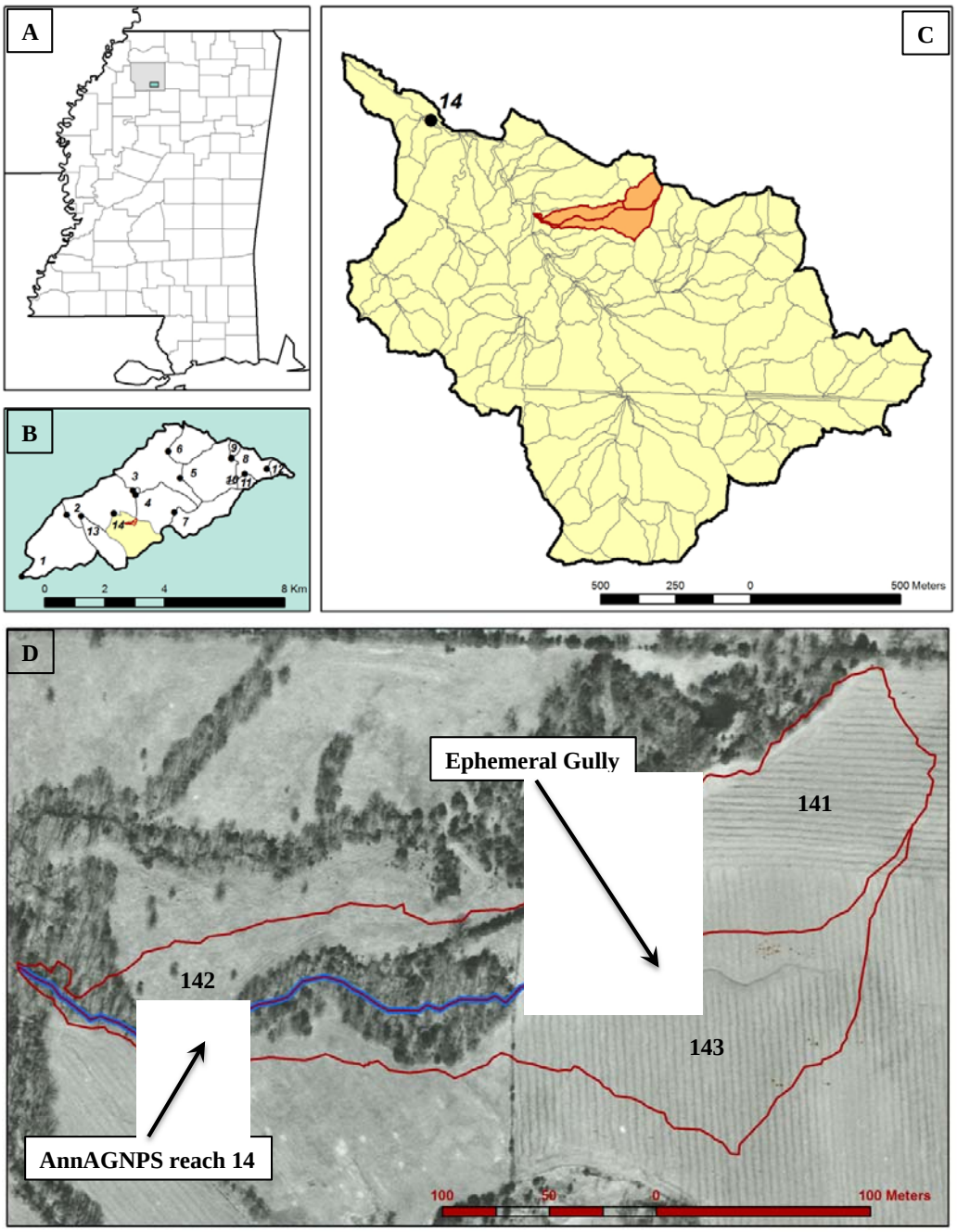


**Figure 7.** Geographical location of the site selected for demonstrating the AnnAGNPS riparian buffer component. The site is located in the State of Mississippi (A) and represents a subset of the Goodwin Creek Experimental Watershed (B). The outlet was selected downstream of station 14 (C) but results are only reported for reach 14 (blue line in D) and for AnnAGNPS cells 141, 142, and 143 (red polygons in D)

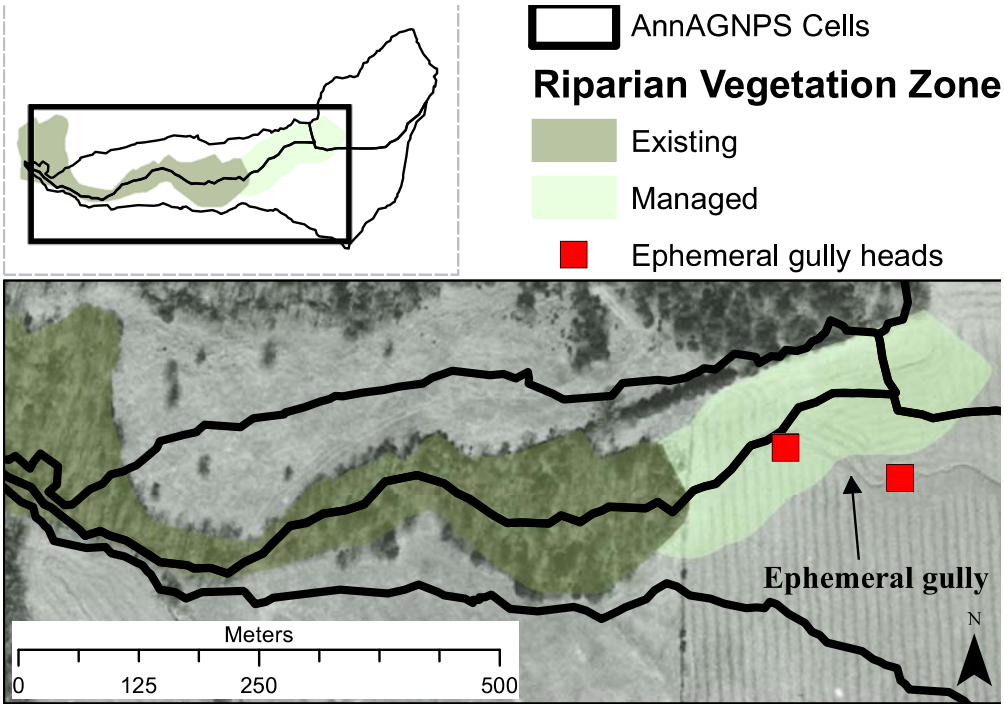


**Figure 8.** Simulated scenarios considered in the evaluation of the vegetation type on the AnnAGNPS riparian buffer component estimation of sediment loads.

705
706

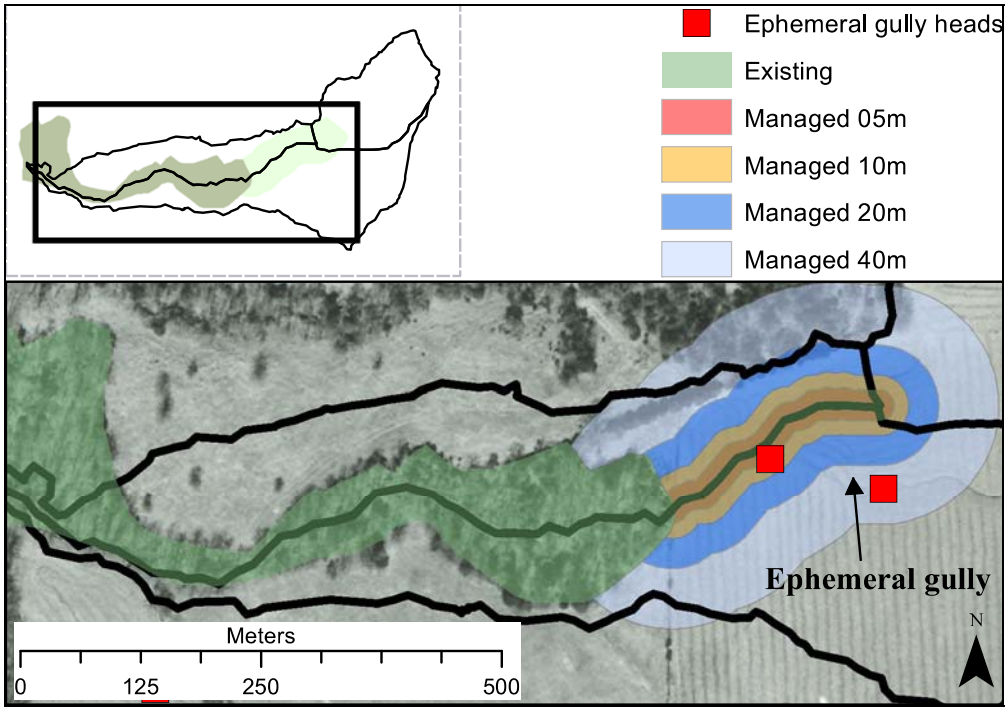


**Figure 9.** Simulated scenarios considered in the evaluation of the riparian buffer width on the AnnAGNPS riparian buffer component estimation of sediment loads.

710
711

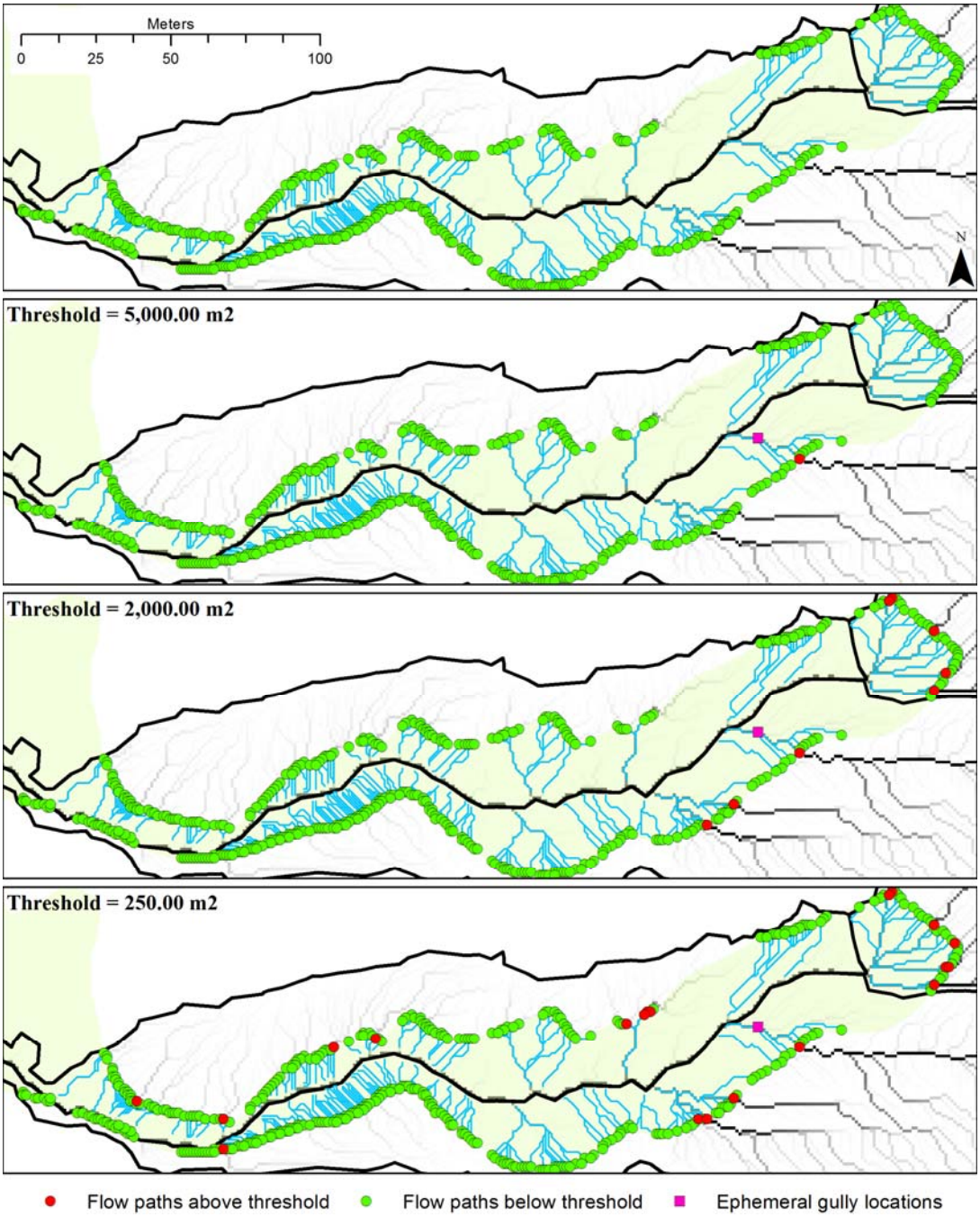


**Figure 10.** Simulated scenarios considered in the evaluation of the presence of concentrated flow paths with high energy (short-circuits) on the AnnAGNPS riparian buffer component estimation of sediment loads.

712

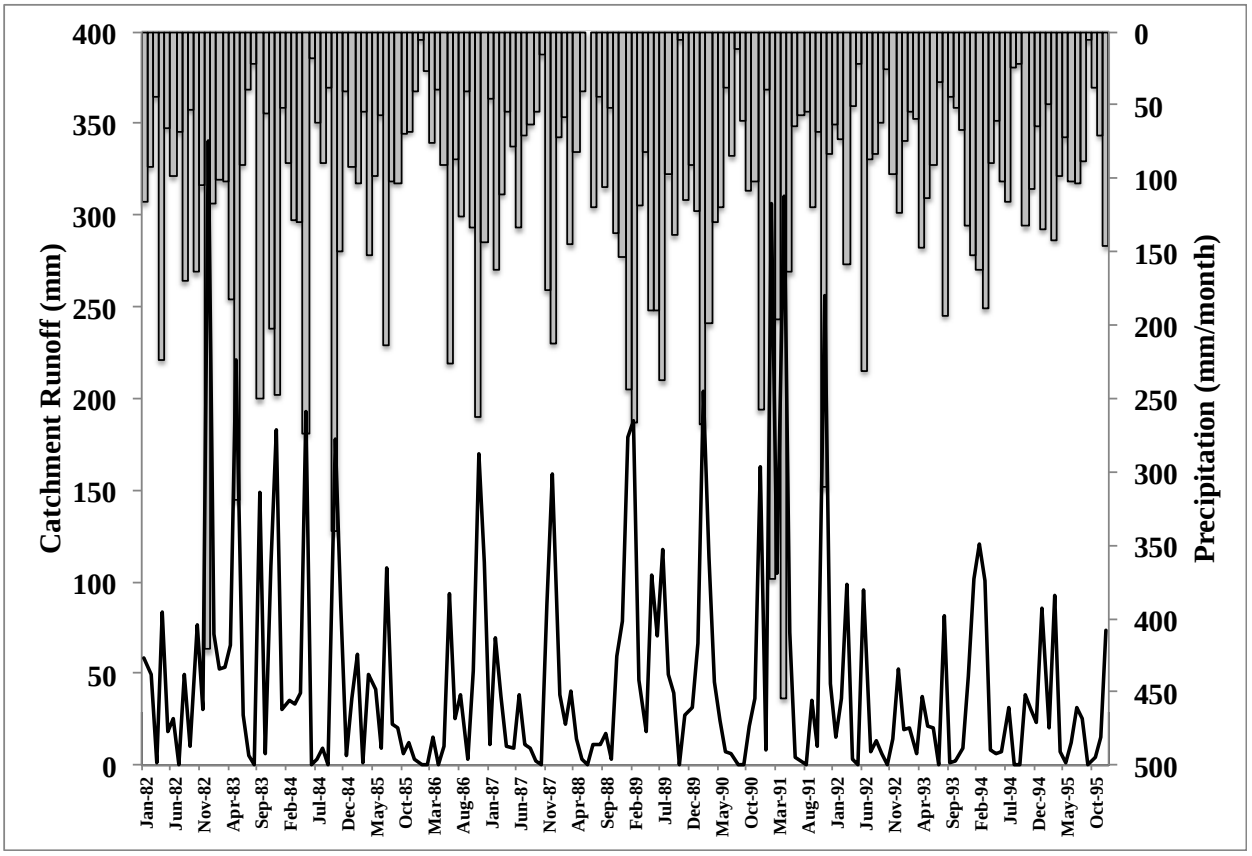


**Figure 11.** Sediment load downstream of reach 14 generated from sheet and rill sources from the AnnAGNPS simulation without riparian vegetation.

716

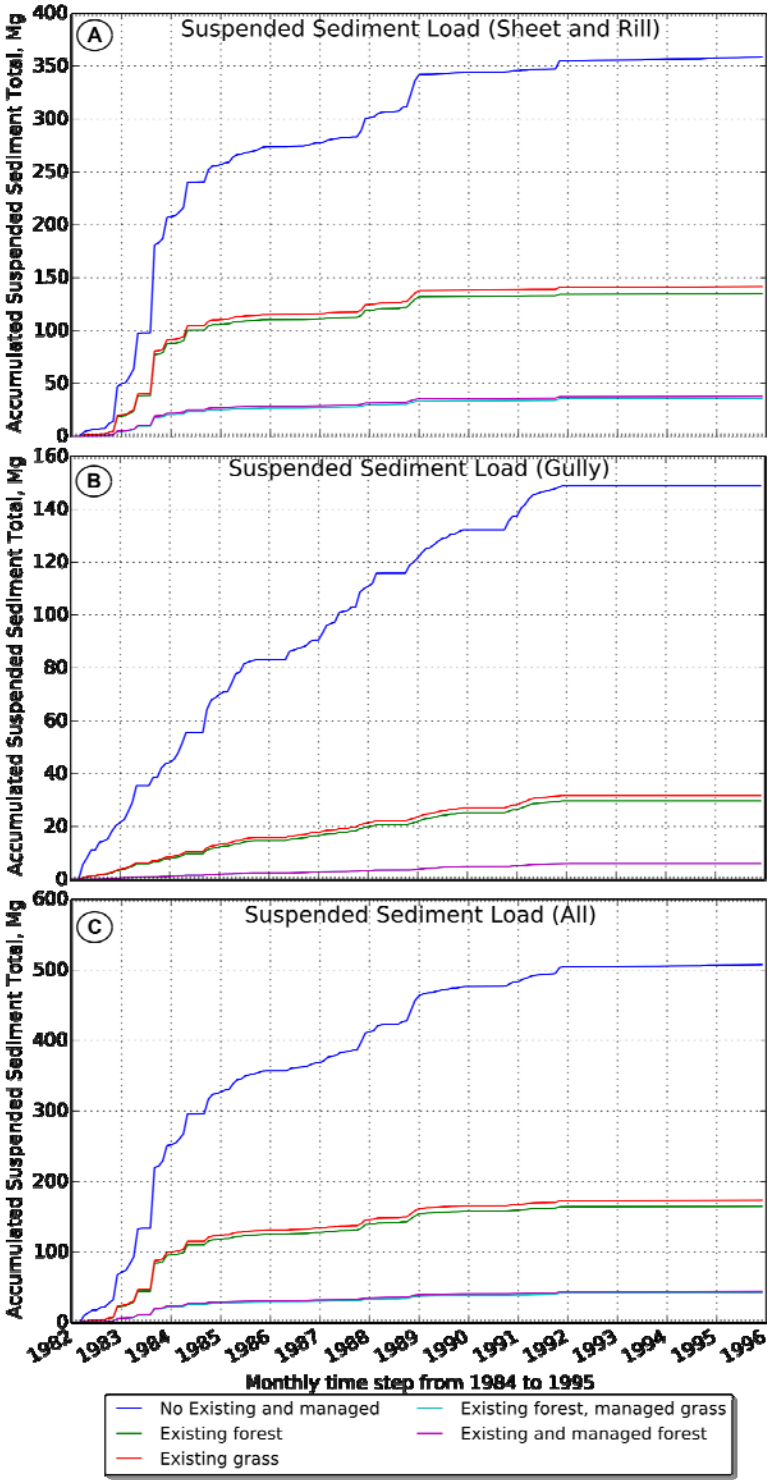


**Figure 12.** Accumulated sediment load downstream of reach 14 generated from sheet and rill (A), ephemeral gully (B), and all combined sources (C) for each of the five simulated vegetation cover type scenarios for the riparian buffer zones.

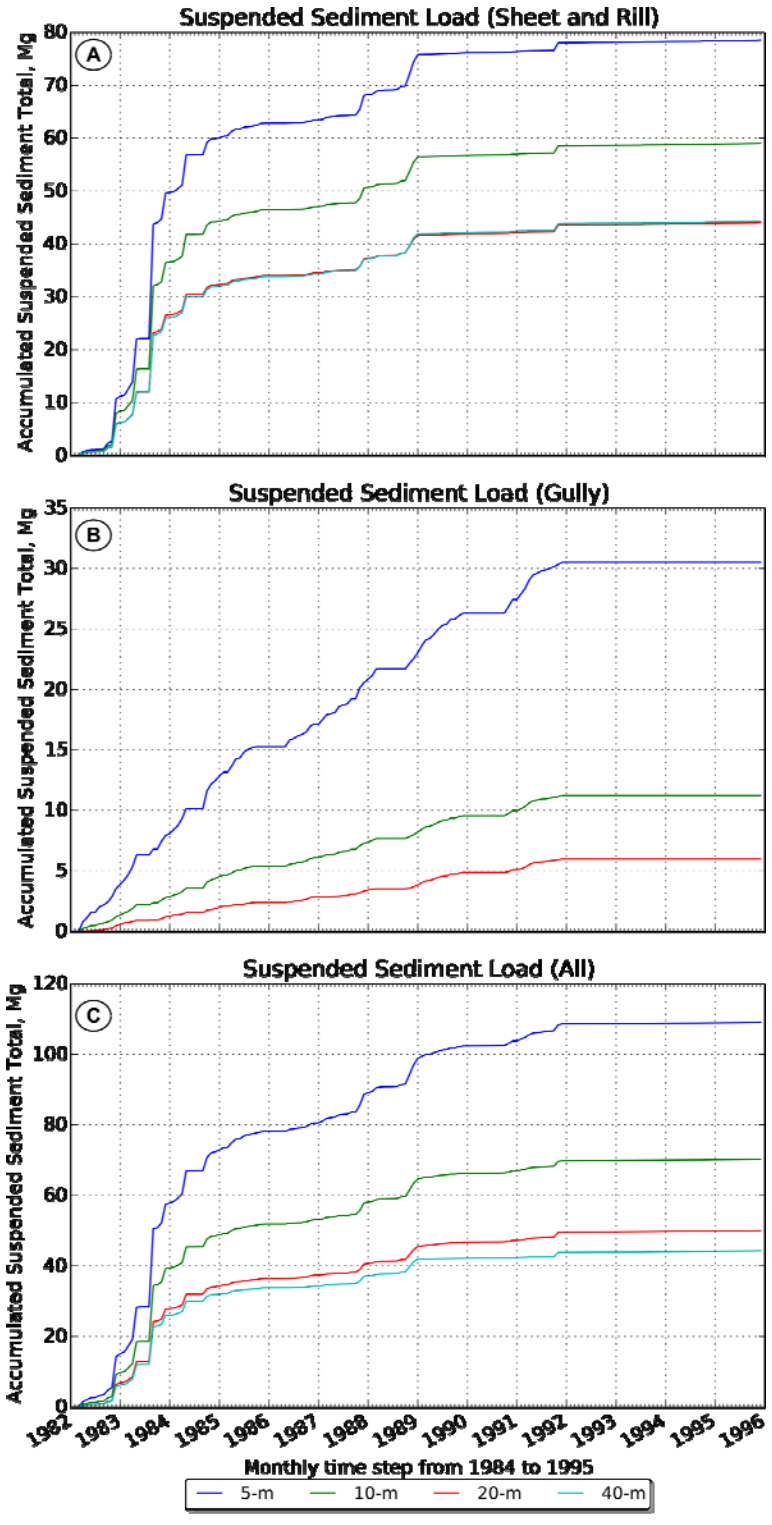


**Figure 13.** Accumulated sediment load downstream of reach 14 generated from sheet and rill (A), ephemeral gullies (B), and all sources (C) for each of the four simulated buffer width scenarios.

720

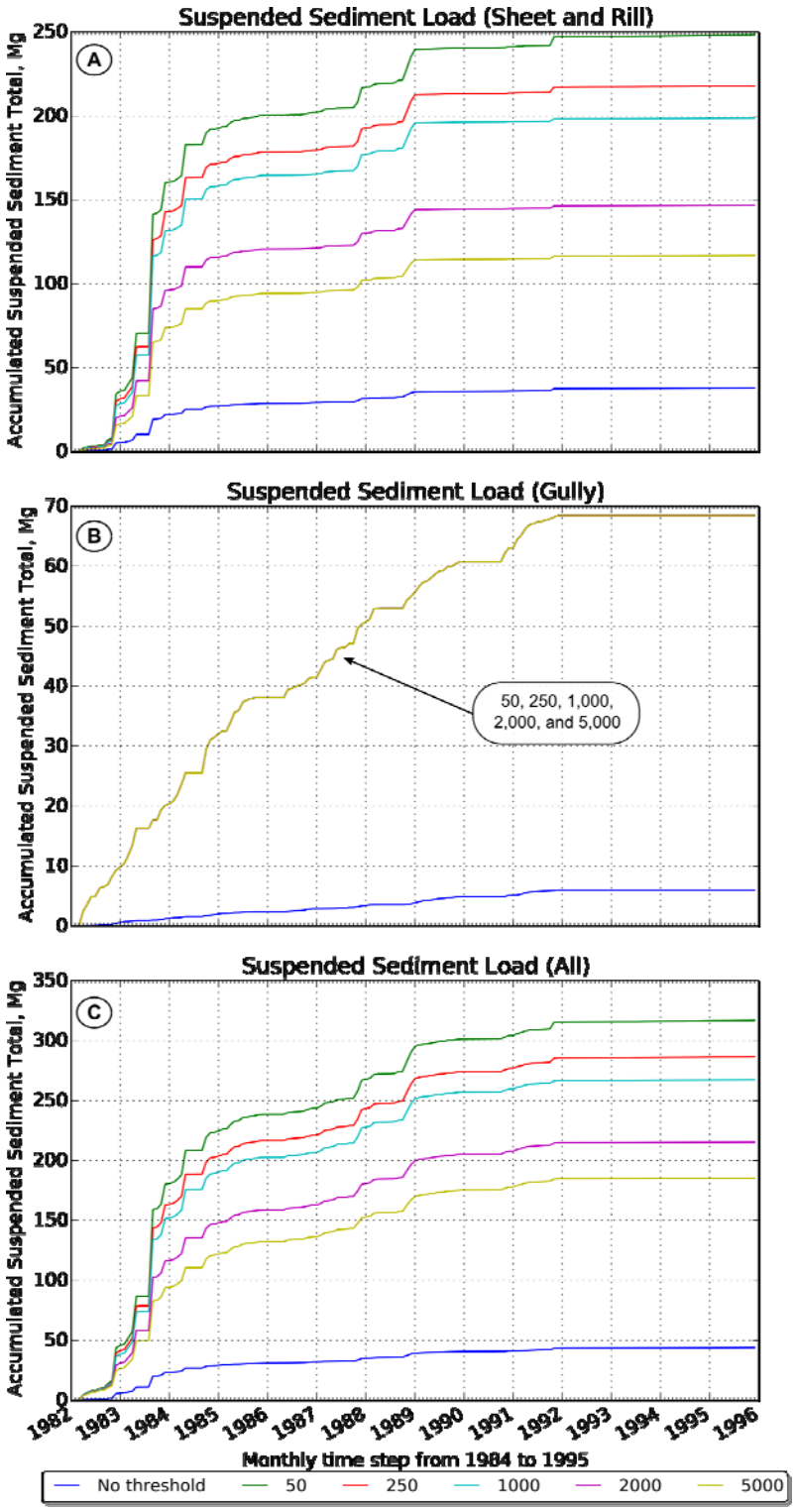


**Figure 14.** Accumulated sediment load downstream of reach 14 generated from sheet and rill (A), ephemeral gullies (B), and all sources (C) for each of the six simulated drainage area thresholds ($m^2$) considered.

721
722